Physiological and Genetic Factors for High Leaf Photosynthetic Capacity in Soybean (*Glycine max* (L.) Merr.)

2019

Kazuma Sakoda

Contents

in soybean

Summary

The enhancement of leaf photosynthesis can be the promising pathway to improve the biomass productivity in soybean (*Glycine max* (L.) Merr.). Targets for enhancing leaf photosynthetic capacity of soybean, however, remain to be elucidated. The objective of the present study is (1) to reveal the natural variation in leaf photosynthetic capacity among various soybean varieties, and (2) to elucidate the genetic and physiological factors responsible for the high capacity for leaf photosynthesis among soybeans.

Firstly, I conducted an initial screening based on the thermal imaging and the gas exchange measurement under the controlled condition with 216 soybean varieties. The subsequent field experiments were conducted for three years using the selected varieties to confirm the variation in leaf photosynthetic capacity under the field condition. A CO_2 assimilation rate (*A*) ranged from 18.1 μmol m^{-2} s^{-1} to 27.6 μmol m^{-2} s^{-1} and PI 594409 A, a soybean cultivar in China, and Jijori, a local cultivar in North Korea, showed extremely high *A* among 34 varieties under the controlled condition. In the field experiment, Jijori consistently showed greater *A* than the other varieties, including three elite varieties in Japan and USA, throughout all the years. In addition, *A* of two varieties, Jin dou 17, a soybean cultivar in China, and Peking, a landrace in China, were comparable with that of

Jijori in 2016 and 2017, respectively. These results confirm that three soybean varieties, Jijori, Jin dou 17 and Peking can have the high capacity for leaf photosynthesis among soybeans.

The A-C_i analysis suggested that the high efficiency of the gas diffusion conductance from the intercellular spaces to the chloroplast (g_m) and/or the CO_2 fixation activity, represented by the maximum rates of carboxylation (Vc_{max}), were exhibited in Jijori, Jin dou17 and Peking. In common, the three varieties with greater A showed higher g_m than the other varieties. The Vc_{max} estimated based on the A-C_c analysis in Jijori was highest among the varieties while that of Jin dou 17 and Peking were lowest or second lowest. Jijori showed the greater content per unit leaf area of nitrogen (N) and ribulose-1,5-bisphosphate carboxylase/oxygenase (Rubisco) due to the higher portion of total soluble protein (TSP) distributed to Rubisco among the varieties, which could contribute to the greater CO_2 fixation activity. In addition, Peking showed greater g_s among studies varieties. These facts suggest that there can be several traits as the target to enhance leaf photosynthetic capacity in soybean, and simultaneous improvement of these traits might realize the drastic enhancement of leaf photosynthetic capacity.

The field experiments were conducted over three years using Enrei, Peking and the chromosome segment substitution lines (CSSLs) derived from their progenies. The

genetic analysis was performed to detect quantitative trait loci (QTLs) responsible for the variation in *A* between Enrei and Peking. Peking stably showed higher *A* than Enrei after the flowering stage. The genetic analysis identified two novel QTLs, which were located on chromosome 13 (*qLPC13*) and 20 (*qLPC20*). The Peking allele at *qLPC13* increased *A* by 8.3% due to greater g_s and mesophyll activity (A/C_i) in the Enrei genetic background, indicating this QTL can be related to high photosynthetic capacity in Peking. In contrast, the Peking allele at *qLPC20* decreased *A* by 15.3% due to the considerable reduction in both of g_s and A/C_i.

The present study identified three soybean varieties with the high capacity for leaf photosynthesis among soybeans. The high photosynthetic capacity of these varieties can be attributed to high g_s, g_m, or Vc_{max}, demonstrating that the several physiological traits can be the promising targets to enhance leaf photosynthetic capacity in soybean. In addition, the genetic analysis using the CSSLs revealed two novel QTLs related to leaf photosynthetic capacity of soybean. The understandings obtained in the present study give us the advanced insight into the physiological and genetic mechanisms underlying leaf photosynthetic capacity of soybean and will open a novel pathway enhancing the photosynthetic capacity towards the yield improvement in soybean breeding.

Chapter 1

Introduction

1.1 Historical perspective of the soybean production

Soybean (*Glycine max* (L.) Merr.) is one of the world's most important crops since it is the main sources of protein and oil for humans and livestock consumption (USDA, 2012). The global production of soybean (334,894 Kt) was the fourth largest after that of maize (*Zea mays* L.) (1,060,107 Kt), wheat (*Triticum aestivum* L.) (749,460 Kt) and paddy rice (*Oryza sativa* L.) (740,961 Kt) in 2016. (Food and Agriculture Organization of the United Nations, 2018). The human population is predicted to increase from 7 billion at the current to 9.5 billion by 2050 (USCB, 2018). The further increase in the crop production is required to meet the food demand from the rapidly growing human population.

The current global production of soybean reaches approximately 335,000 Kt, and more than 80% of total production is provided by three counties, United State of America (USA) (117,208 Kt), Brazil (96,297 Kt) and Argentine (58,799 Kt) (Food and Agriculture Organization of the United Nations, 2018). The soybean production in these countries has been continuously increased in the past 50 years, which could be achieved by the

expansion of the production area and the increase in the seed yield per unit of the production area (Masuda and Goldsmith, 2009). In USA, an averaged seed yield had linearly increased from 1690 kg ha^{-1} in 1961 to 2823 kg ha^{-1} in 2011 with the annual gain of 27.0 kg ha^{-1}. The continuous increase in the soybean yield has been attained by the improvement of the management practice (e.g., earlier planting, higher plant density, better weed control, and lower harvesting loss), the rising CO_2 level of the atmosphere and the genetic improvement of soybean (Specht et al., 1999). It was shown that the decrease in plant height through the breeding process strengthened the lodging tolerance, which resulted in the higher yield in modern soybean varieties than old varieties released in Canada and China (Morrison et al., 2000; Jin et al., 2010; Liu et al., 2012). The introduction of the transgenic soybean which has the herbicide tolerance has accelerated the improvement of the soybean yield after 1996 (Ainsworth et al., 2012). In addition to these events, the enhancement of the yield potential (Y_p) have had the great contribution to the yield improvement in soybean. The elucidation of the genetic and physiological mechanisms underlying the Y_p enhancement can contribute to the development of the breeding strategy for the further improvement in the soybean yield.

1.2 Mechanisms underlying the improvement of soybean yield potential

The Y_p is defined as a crop yield that can be achieved when the crop is grown under an adapted environment and favorable conditions where biotic and abiotic stresses are effectively controlled. According to the principles of Monteith (1977), the crop Y_p at a given location can be determined as a combining product of an annual integrated incident of the solar radiation, an efficiency with which that radiation is intercepted by crop plants (ε_i), an efficiency with which the intercepted radiation is converted to a biomass (ε_c), and a partitioning ratio of the biomass into seeds (ε_p). Historical analysis using the soybean varieties which had been released in the past several decades showed that ε_i, ε_c, and ε_p had continuously increased through the breeding process in Canada, China and USA (Morrison et al., 2000; Jin et al., 2010; Liu et al., 2012; Koester et al., 2014). These previous studies indicated that the increase in the seed number per plant (i.e. the increase in ε_p) was a major factor responsible for the increase in the seed yield. Zhu et al., (2010) concluded that the further increase in ε_i and ε_p can be unexpectable since these parameters have mostly reached a theoretical maximum value at the central Illinois in USA. On the other hand, ε_c has reached less than half of the theoretical maximum value, which means that there is still a room to increase ε_c, furthermore. The ε_c is depended largely on an accumulative amount of a CO_2 assimilation occurred at individual leaves in the crop canopy. Previous studies have evidenced a positive correlation between a CO_2

assimilation rate (*A*) and the seed yield in soybean (Buttery et al., 1981; Jin et al., 2010; Liu et al., 2012). In addition, free-air CO_2 enrichment (FACE) experiments revealed that elevated [CO_2] caused the simultaneous increase in *A* and the seed yield among C_3 crops, including soybean (Mitchell et al., 1999; Ainsworth and Long, 2005). Long et al., (2006), considering these facts, identified an enhancement of leaf photosynthetic capacity as a promising strategy to improve the soybean yield.

1.3 Strategy for enhancing leaf photosynthetic capacity in soybean

The natural variation in *A* within or among crop species can be utilized to improve *A* by elucidating the mechanisms underlying such variation (Flood et al., 2011). The significant variation in *A* has been revealed among rice varieties (Kawamitsu and Agata, 1987; Kanemura et al., 2007; Ohsumi et al., 2007). Takanari, the high-yielding indica variety in Japan, was shown to have high *A* among various rice cultivars, and the genetic and physiological factors related to high capacity in Takanari has been elucidated (Takai et al., 2013). Previous studies have also revealed the large variation in *A* among various soybean varieties (Ojima et al., 1972; Butterry et al., 1977; Tanaka et al., 2010; Liu et al., 2012; Koester et al., 2016; Tomeo et al., 2017). Most of the previous studies on soybean photosynthesis were conducted with the limited populations of commercial varieties

released in Canada, China, Japan, or USA. It is, thus, desired to evaluate leaf photosynthetic capacity among untapped soybean population with the high genetic diversity, which is expected to hold a novel variety with the high capacity for leaf photosynthesis.

Leaf photosynthesis is considered as a combined process of supplying CO_2 from the atmosphere to the chloroplast and the fixation of CO_2 at the chloroplast. Previous studies have shown a strong correlation between A and a stomatal conductance (g_s), a gas diffusion efficiency via the stomata under high light conditions in several crop species (Fischer et al., 1998; Ohsumi et al., 2007; Tanaka et al., 2010). The potential of g_s can be determined by the size, depth, density, and opening of a single stoma (Franks and Breeling, 2009). According to the biochemical model for photosynthesis, A is mainly determined by either a carboxylation of ribulose-1,5-bisphosphate (RuBP), a regeneration of RuBP or an availability of triose phosphate in the chloroplast, depending on an intercellular [CO_2] (C_i) (Farquhar et al., 1980; Sharkey, 1985). At the current atmospheric [CO_2], CO_2 fixation may be limited by the carboxylation of RuBP, catalyzed by Rubisco in plants. The content per unit leaf area and the kinetic properties of Rubisco have been shown as a determinant of A in rice at the current [CO_2] (Makino et al., 1985). The N content per unit leaf area has also been demonstrated to correlate with A among several crop species since

15–30% of total N can be distributed to Rubisco in C_3 plant species (Evans, 1983; Evans, 1989; Sinclair and Horie, 1989). In brief, physiological factors, represented by the biochemical and morphological characteristics, can be a determinant of leaf photosynthetic capacity in crop species. These physiological factors can be, furthermore, governed by the genetic and environmental factors (Flood et al., 2011). It is worth noting that *NAL1* and *CAR8* were identified as the causal genes for the variation in *A* among rice varieties (Takai et al., 2013; Adachi et al., 2017). The genetic factors controlling the variation in *A*, on the other hand, has remained unclear in field-grown soybeans, although a few studies have reported the genetic factors in pot-grown soybeans (Vieira et al., 2006; Yin et al., 2010; Li et al., 2016). Thus, the elucidation of the genetic and physiological factors related to the high capacity for leaf photosynthesis in field-grown soybeans can provide a novel strategy to exploit with soybean breeding.

1.4 The objective and outline of the present study

The objective of the present study is (1) to reveal the natural variation in leaf photosynthetic capacity among various soybean varieties, and (2) to elucidate the genetic and physiological factors responsible for the high capacity for leaf photosynthesis among soybeans.

Firstly, I aimed to identify a novel soybean variety with the high capacity for leaf photosynthesis (Chapter 2). The gas exchange measurement was conducted under the controlled condition in 34 varieties expected to cover the wide variation in *A* among soybeans. The subsequent field experiments were also conducted with the selected varieties to confirm the variation in *A* under the field condition. Secondary, I aimed to elucidate the physiological factors related to the high capacity for leaf photosynthesis among soybeans (Chapter 3). In chapter 2, I identified three varieties of soybean, Jijori, a cultivar in North Korea, Jin dou 17, a cultivar in China, and Peking, a landrace from China, which showed high *A* among soybeans. The gas exchange measurements as well as the biochemical and morphological analyses were conducted among the selected varieties. Thirdly, I aimed to elucidate the genetic factors related to the high capacity for leaf photosynthesis among soybeans (Chapter 4). In chapter 2, I reveled greater *A* of Peking than Enrei, a leading variety in Japan, after the flowering stage under the field condition. The gas exchange measurements were conducted to evaluate *A* among Enrei, Peking and the CSSLs derived from their progenies, while the genetic analysis was performed to detect QTLs responsible for the variation in *A* between Enrei and Peking. Finally, I integrated all the results obtained in Chapter 2 to 4 and discussed the potential and strategy for the genetic improvement of leaf photosynthetic capacity of soybean at the current and

future environment (Chapter 5).

Chapter 2

Natural variation in leaf photosynthetic capacity among Asian varieties of soybean

2.1 Introduction

The large variation in *A* within or among crop species can be exploited to improve *A* by elucidating the mechanisms underlying such variation (Flood et al., 2011). Previous studies have revealed the large variation in *A* among soybean varieties (Ojima et al., 1972; Butterry et al., 1977; Tanaka et al., 2010; Liu et al., 2012; Koester et al., 2016; Tomeo et al., 2017), although these studies were conducted with the limited populations of the soybean varieties released in Canada, China, Japan, or USA. It is, thus, desired to evaluate leaf photosynthetic capacity among untapped soybean population with the high genetic diversity, which is expected to hold a novel variety with the high capacity for leaf photosynthesis.

To evaluate the natural variation in leaf photosynthetic capacity among the soybean varieties, I randomly selected 216 varieties from the soybean germplasm collection developed by Ray et al., (2015). Most of the varieties are originated from various Asian countries and provinces and belong to maturity ground IV. I conducted the preliminary

selection based on leaf temperature measurements as described in Tanaka et al., (2013a), to establish a sub collection for the present study. This sub collection contains 34 varieties, and consists of 16 varieties with high leaf temperature, 16 varieties with low temperature, and two commercial varieties as the reference. This sub collection was expected to cover the wide range of the natural variation in leaf photosynthetic capacity among soybeans.

In Chapter 2, I aimed to identify a novel soybean variety with the high capacity for leaf photosynthesis among soybeans. To reach this objective, an initial analysis based on *A* was conducted in 34 soybean varieties under the controlled condition to screen the candidates of the variety with high *A*. The subsequent field experiments were conducted to confirm the variation in *A* under the field condition.

2.2 Materials and methods

2.2.1 Materials and cultivation of soybean plants

I conducted the chamber experiment with 34 soybean varieties (Table S1.1) screened by the preliminary evaluation of leaf temperature. These varieties were sown in 3 L pots containing potting soil (Sunshine Mix #1 LC1, SunGro Horticulture, Agawam, MA, USA) with a top dressing of Osmocote (Scotts Miracle-Gro, Marysville, OH, USA). It was reported that Tachinagaha (PI 594287), a commercial variety in Japan, showed lower

photosynthetic capacity than Stressland, a commercial variety in USA (Tanaka et al., 2008). Kawasaki et al., (2016) reported that UA 4805 (PI 639187), a commercial variety in USA, showed higher biomass productivity than Japanese cultivars including Tachinagaha. UA 4805 also showed higher g_s among Japanese and USA commercial varieties, which could result in higher capacity for leaf photosynthesis (Tanaka et al., 2010). Based on these facts, Tachinagaha and UA 4805 were used as reference cultivars in in the chamber experiment. The 34 varieties belong to maturity group four to five and most of them show a determinate type in the stem growth habit. Five pots were prepared per each variety and each pot had one plant. The pots were placed randomly and grown in a growth chamber (Conviron, Winnipeg, Manitoba, Canada) with the day/night temperature set to 26°C/20°C and a photoperiod of 14h. The light intensity was set to a PPFD of 1200 μmol m^{-2} s^{-1} at plant height. Plants were watered and fertilized as needed.

The field experiments were conducted at the Experimental Farm of the Graduate School of Agriculture, Kyoto University, Kyoto, Japan (Lat. 35°2′N, Long. 135°47′E, and 65 m altitude; Fluvic Endoaquepts soil type) in 2014, 2016 and 2017. I used four varieties, PI 594409 A, PI 603911 C, Tachinagaha, UA 4805, in 2014, 11 varieties, Enrei, Fukuyutaka, LD-003309, NC-Raleigh, Peking, PI 594409 A, PI 603911 C, Stressland, Tachinagaha, UA 4805 and UA 4910 in 2016 and 10 varieties, Enrei, Peking, PI 404159,

PI 407832 B, PI 458098, PI 592940, PI 594409 A, PI 603911 C, UA 4805 and UA 4910 in 2017, respectively. These varieties include the Japanese and USA commercial varieties reported high yielding. Tachinagaha and UA 4805 were used as reference varieties in 2014 and 2016. The sowing date was 25 June in 2014, 4 July. in 2016 and 27 Jun. in 2017. The row and plant spacing distances were 0.7 m and 0.2 m in 2014, and 0.7 m and 0.15 m in 2016 and 2017, respectively. The N, P_2O_5, and K_2O fertilizers were applied at 3, 10, and 10 g m^{-2}, respectively, before the sowing. I established two replicates of the experimental plot in 2014 and single plot in 2016 and 2017 for each variety. Each experimental plot was composed of 33 plants in three rows in 2014, 24 plants in two rows in 2016 and 48 plants in four rows in 2017, respectively. I recorded days after planting (DAP) when each soybean variety reached the beginning of the flowering (R1) and the seed filling (R5) in all the years.

2.2.2 Gas exchange measurements

The characteristics of leaf photosynthesis were evaluated in the soybean varieties using a portable gas-exchange system LI-6400 (*LI-COR*, Lincoln, NE, USA) in the chamber experiment and the field experiments in 2014 and 2016, and LI-6800 (*LI-COR*, Lincoln, NE, USA) in 2017, respectively. In the chamber experiment, A, g_s and C_i were measured

with a CO_2 concentration of 380 µmol mol^{-1}, a PPFD of 2000 µmol m^{-2} s^{-1}, and an air temperature of 26°C at the uppermost fully expanded leaf at 26 DAP when the plants were almost at the 4th trifoliate stage (n = 3).

In the field experiments in 2014 and 2016, A, g_s and C_i were measured with a CO_2 concentration of 400 ppm, a PPFD of 2000 µmol m^{-2} s^{-1} in 2014 or 1500 µmol m^{-2} s^{-1} in 2016 and 2017 at the uppermost fully expanded leaf from 8:30 to 13:00 on the sunny day. An air temperature in the chamber was set on 33°C in 2014 and 2016, and on 35°C in 2017. The mesophyll activity was evaluated as the ratio of A to C_i (A/C_i). The gas exchange measurements were conducted at 33, 57, 65, and 72 DAP in 2014, at 36, 43, 49 and 59 DAP in 2016, and at 43, 46, 51 and 58 DAP in 2017, respectively. The measurement replication for each line was 8–10 in 2014, 5–6 in 2016 and 4 in 2017.

2.2.3 Statistical analysis

In the chamber experiment, the variation in A among 34 varieties was evaluated by the Tukey-Kramer test. In the field experiments, one-way ANOVA or the Tukey-Kramer test were applied to evaluate the variation in A among the varieties. Statistical analyses were conducted using R (R Foundation for Statistical Computing, Vienna, Austria.).

2.3 Results

In the chamber experiment, leaf photosynthetic capacity was evaluated among the 34 varieties at the 4th trifoliate stage under the controlled condition. The *A* ranged from 18.1 µmol m^{-2} s^{-1} in PI 398406 to 28.7 µmol m^{-2} s^{-1} in PI 594409 A (Fig. 2.1). The *A* of PI 603911 C was the second highest among all the genotypes, and it was 27.2 µmol m^{-2} s^{-1}.

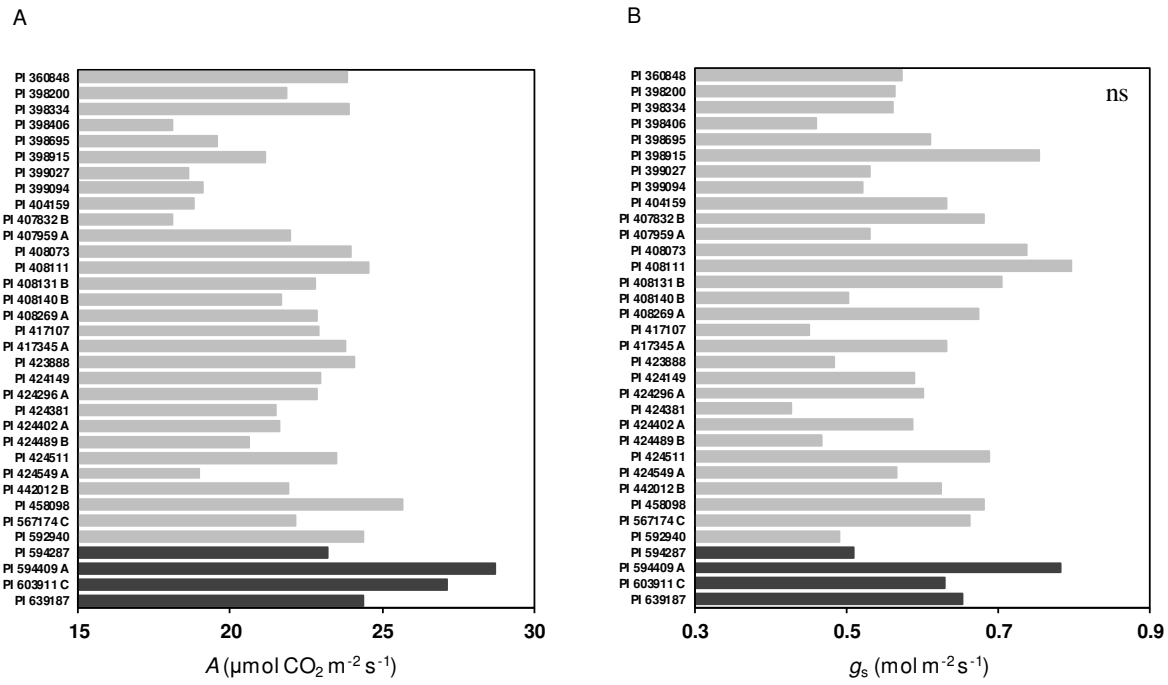

Fig. 2.1 Variation in the CO_2 assimilation rate (*A*) and stomatal conductance (g_s) among 34 soybean varieties.

ns means there is no significant difference among 34 soybean varieties.

According to the Tukey-Kramer test, *A* of PI 594409 A was significantly higher than six varieties while that of PI 603911 C was significantly higher than two varieties ($p < 0.05$).

The *A* of PI 594409 A and PI 603911 C were greater by over 10% than two reference cultivars, Tachinagaha and UA 4805. The g_s varied from 0.43 mol m^{-2} s^{-1} in PI 424381 to 0.78 mol m^{-2} s^{-1} in PI 408111. There was no significant difference of g_s among all the varieties. The g_s of PI 594409 A was the second highest of all the varieties, while that of PI 603911 C was intermediate.

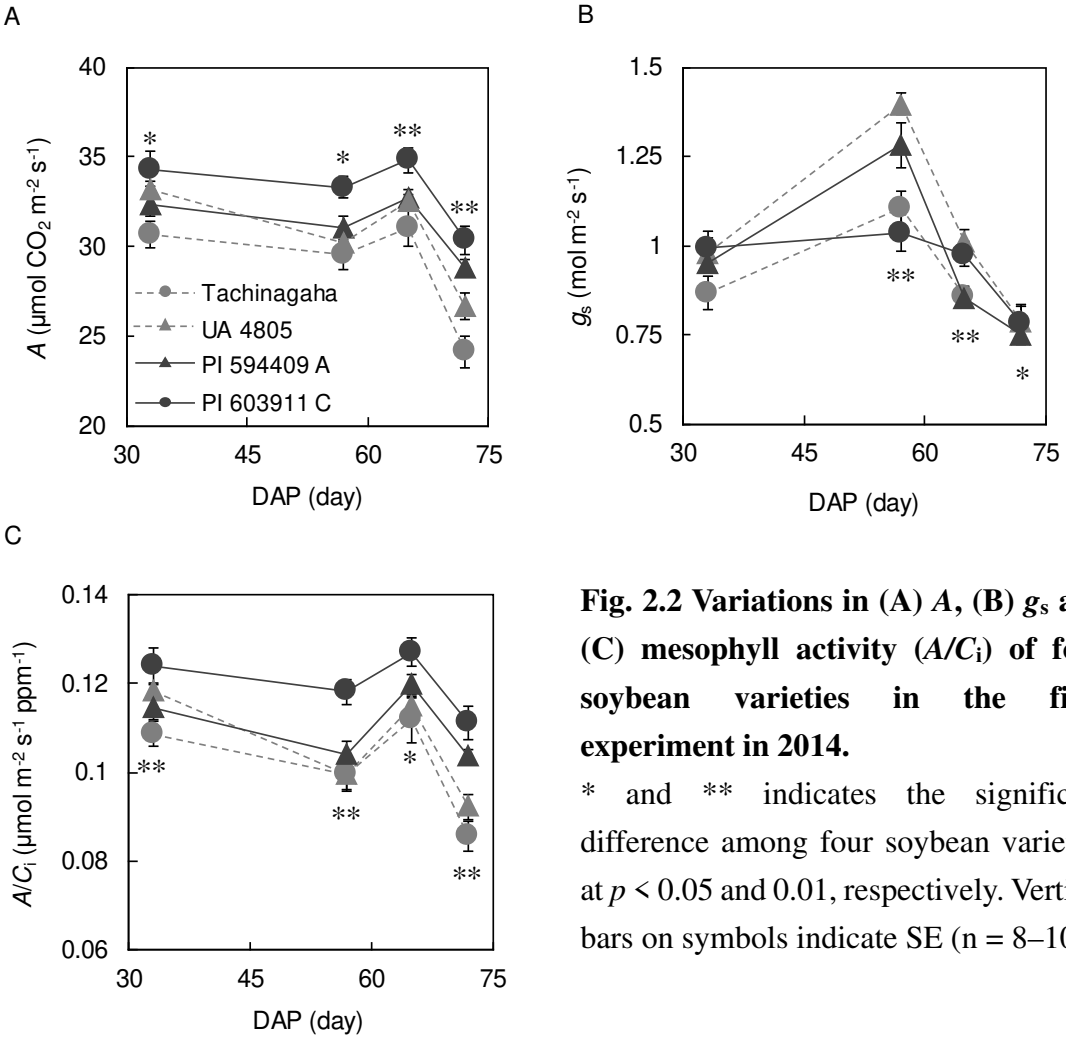

Fig. 2.2 Variations in (A) *A*, (B) g_s and (C) mesophyll activity (A/C_i) of four soybean varieties in the field experiment in 2014.

* and ** indicates the significant difference among four soybean varieties at $p < 0.05$ and 0.01, respectively. Vertical bars on symbols indicate SE (n = 8–10).

In the field experiments, leaf photosynthetic capacity was evaluated several times after the flowering stage in soybean varieties. The *A* and A/C_i of PI 603911 C were consistently

highest of the four varieties at all the stages in 2014 (Fig. 2.2). At 65 DAP, *A* of PI 603911 C was 34.8 µmol m^{-2} s^{-1}, which was 11% higher than that of the reference cultivar, Tachinagaha. On the other hand, *A* was similar in PI 594409 A and UA 4805 at all the stages. There was no clear trend in the variation in g_s among the four varieties. There was a significant variation in *A*, g_s, and A/C_i among four varieties throughout all the stages except for g_s at 33 DAP ($p < 0.05$).

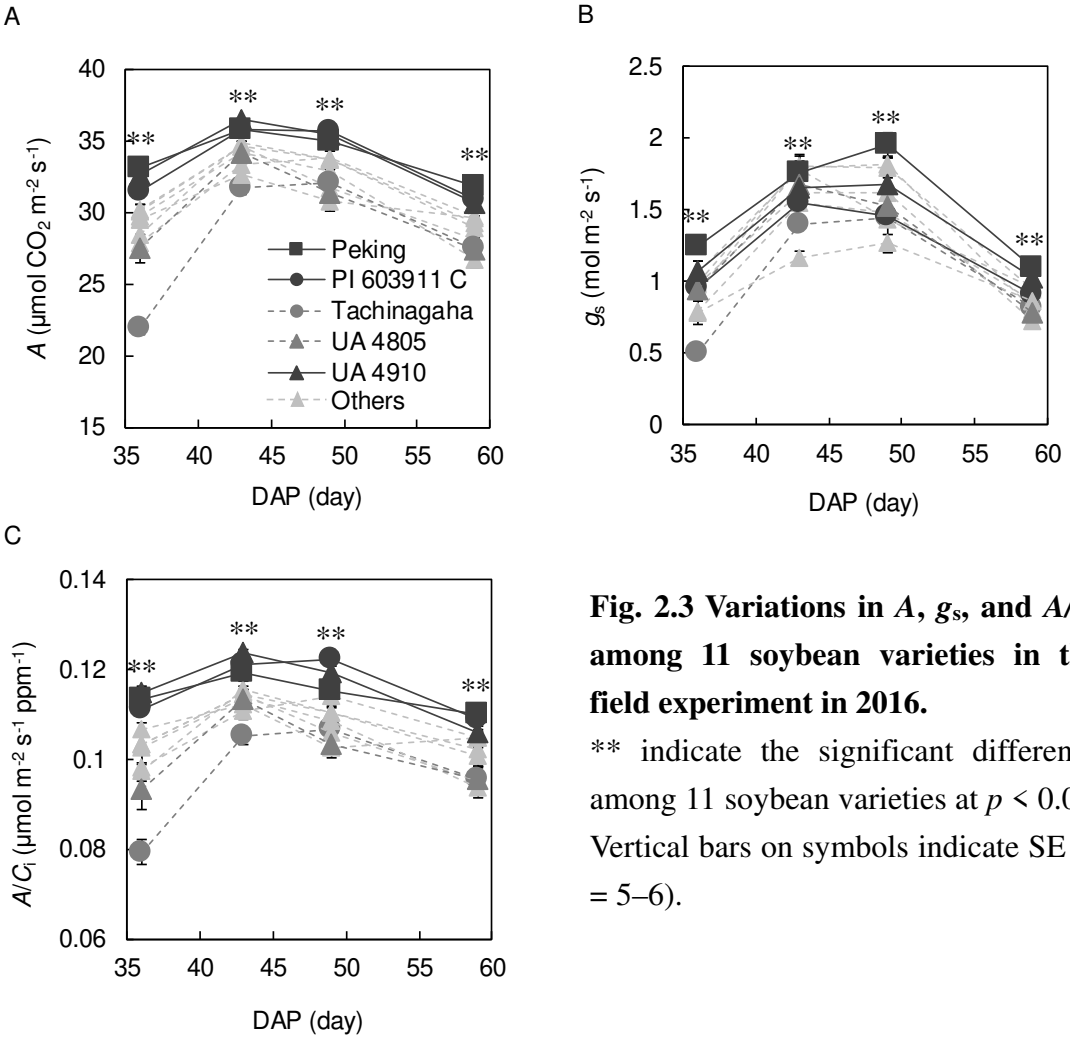

Fig. 2.3 Variations in *A*, g_s, and A/C_i among 11 soybean varieties in the field experiment in 2016.

** indicate the significant difference among 11 soybean varieties at $p < 0.01$. Vertical bars on symbols indicate SE (n = 5–6).

In 2016, the variations in *A*, g_s and A/C_i among 11 varieties were significant throughout

all the stages ($p < 0.01$) (Fig. 2.3). PI 603911 C showed the highest or second highest *A* of 11 varieties including two reference varieties, Tachinagaha and UA 4805, at all the stages. In addition, Peking, a landrace in China, and UA 4910, a high-yielding variety in USA, showed comparable *A* with PI 603911 C at all the stages. The *A* of PI 603911 C, Peking and UA 4910 was higher by 14.8%, 20.6% and 19.0% than UA 4805 at 36 DAP. The g_s of Peking was constantly highest of all the varieties except for 43 DAP, while that of PI 603911 C and UA 4910 was intermediate. The A/C_i of PI 603911 C, Peking and UA 4910 was higher than the others at all the stages.

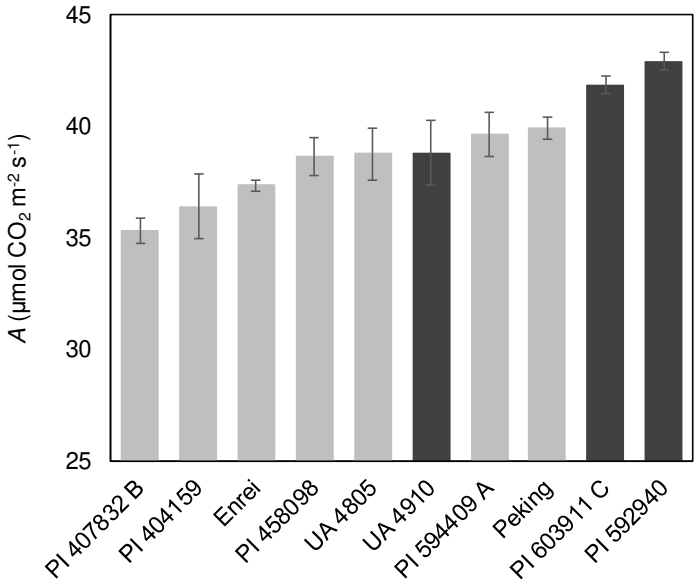

Fig. 2.4 Variation in *A* among 10 soybean varieties in the field experiment in 2017. Columns of three soybean varieties which showed highest *A* in 2016 were colored with black. Vertical bars on each column indicate SE (n = 4).

In 2017, *A* ranged from 35.3 μmol m^{-2} s^{-1} in PI 407832 B, a variety in South Korea, to 42.9 μmol m^{-2} s^{-1} in PI 592940, a variety in China, among 10 varieties at 43 DAP (Fig.

2.4). PI 603911 C and Peking showed second highest *A* of all the varieties at this stage. Based on this result, I selected the five varieties, PI 407832 B, a variety in China, Enrei, a commercial variety in Japan, Peking, PI 592940 and PI 603911 C, to cover the wide variation in *A* among soybeans and evaluated *A* in the five varieties at 46, 51 and 59 DAP.

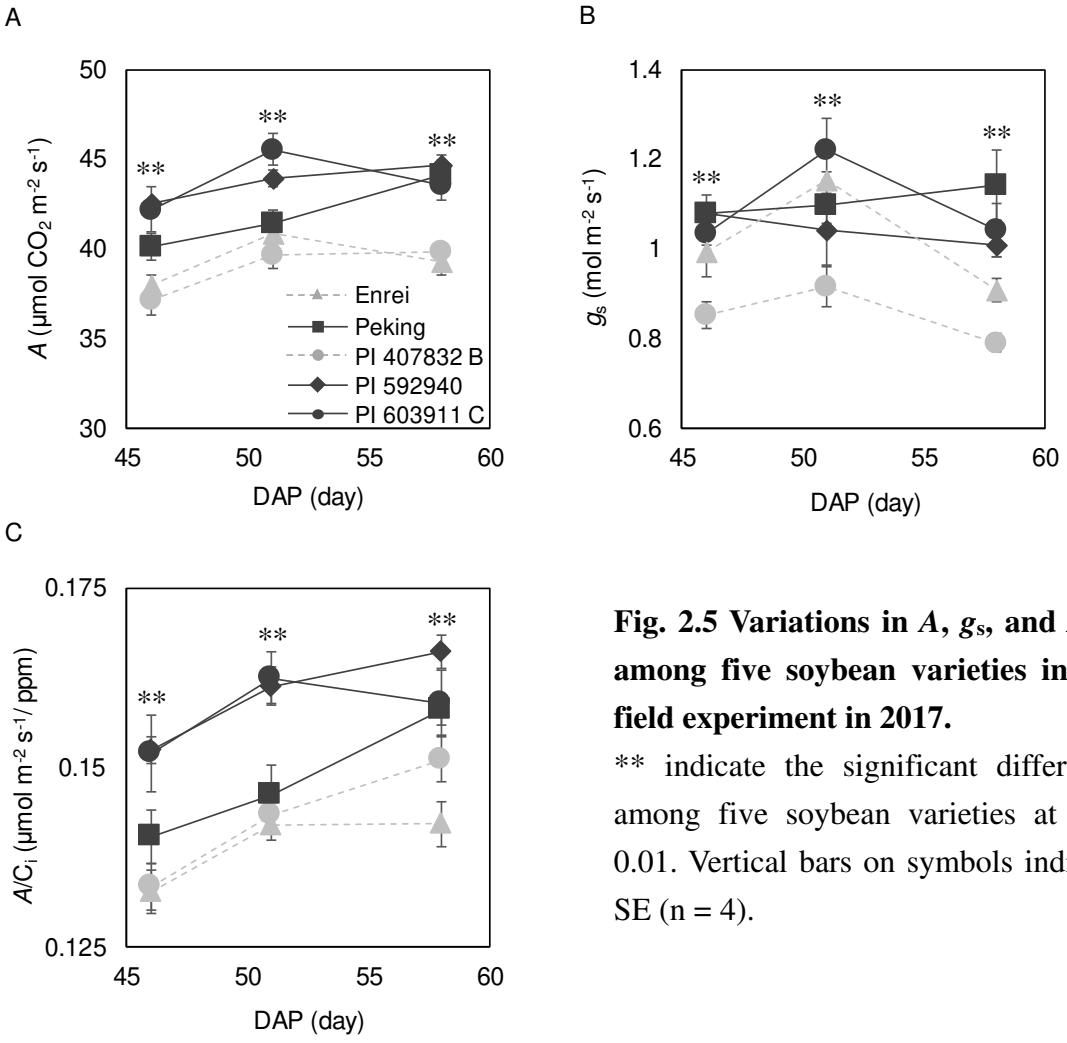

Fig. 2.5 Variations in *A*, g_s, and A/C_i among five soybean varieties in the field experiment in 2017.

** indicate the significant difference among five soybean varieties at $p < 0.01$. Vertical bars on symbols indicate SE (n = 4).

The *A* of PI 592940 and PI 603911 C was comparable and it was significantly higher than Enrei and PI 407832 B at all the stages in 2017 ($p < 0.05$). At 58 DAP, *A* of Peking was

comparable with PI 592940 and PI 603911 C, and it was significantly higher than Enrei and PI 407832 B ($p < 0.05$), whereas there was no significant variation in A among Peking, Enrei and PI 407832 B at 46 and 51 DAP (Fig. 2.5). The g_s of Peking was highest of all the varieties at 46 and 58 DAP, and it was significantly higher than PI 407832 B. The g_s of PI 592940 and PI 603911 C was significantly higher than that of PI 407832 B at 46 and 58 DAP, while there was no significant variation in g_s among PI 592940, PI 603911 C and Enrei at all the stages. PI 592940 and PI 603911 C showed significantly higher A/C_i than Enrei and PI 407832 B through all the stages except for 58 DAP when there was no significant variation in A/C_i between PI 407832 B and PI 603911 C. There was no significant variation in A/C_i among Enrei, Peking and PI 407832 B at 46 and 51 DAP, while there was significant variation between Enrei and Peking at 58 DAP.

2.4 Discussion

Several studies have reported the significant variation in leaf photosynthetic capacity among soybeans (Dornhoff et al., 1970; Ojima, 1972; Buttery et al., 1981; Morrison et al., 2000; Jin et al., 2010; Liu et al., 2012). The linear increase of the soybean photosynthetic rate was reported against year of release, and newer cultivars had up to 23% greater photosynthetic rate than older cultivars (Koester et al., 2016). In this study,

the photosynthetic rate varied more than 50% among 34 varieties under the controlled condition (Fig. 2.1). These results suggest that there is a considerable variation in leaf photosynthetic capacity not only among historical cultivars but also among the exotic varieties of soybean.

The relative levels of leaf photosynthetic capacity among PI 603911 C, Tachinagaha and UA 4805 were conserved across the chamber experiment and the field experiments in 2014 and 2016 (Figs. 2.1, 2.2 and 2.3). PI 603911 C consistently showed greater photosynthetic capacity than the others after the flowering stage in all the years (Figs. 2.2, 2.3 and 2.4). Moreover, Peking and PI 592940 showed comparable *A* with PI 603911 C in 2016 and 2017, respectively. These results confirmed that they have high capacity for leaf photosynthesis among soybeans. Peking is a landrace in China, PI 592940 is a variety in China and named as Jin dou 17, PI 603911 C is a variety in North Korea and named as Jijori. Three variety can be the promising candidates for identifying the mechanism underlying high capacity for leaf photosynthesis in soybean. The *A* values of PI 594409 A were highest among all the soybean varieties in the chamber experiment due to higher g_s. On the other hand, *A* of PI 594409 A was similar to that of UA 4805, one of the reference varieties, in all the field experiments. This was because g_s was almost similar or lower in PI 594409 A comparing with UA 4805 in the field experiments, and PI 594409

A had no advantage that would allow it to achieve high photosynthetic rate. In addition, differences in the environmental conditions and the growth stages of the plants can be the cause of the inconsistency of the variation in *A* between the chamber experiment and the field experiments.

Leaf photosynthetic capacity is determined by both the CO_2 supply from atmosphere to the chloroplast and the CO_2 fixation at the chloroplast (Farquhar et al., 1980). It is well known that g_s strongly affects leaf photosynthetic capacity (Farquhar and Sharkey, 1982). Ohsumi et al. (2007) reported that g_s was one of the major factors determining the variation in leaf photosynthetic capacity among rice varieties. A positive correlation between *A* and g_s has been observed among several crop species (Fischer et al., 1999; Ohsumi et al., 2007; Tanaka et al., 2008). This correlation was not observed among the 34 varieties of soybean in the chamber experiment (data not shown). In the field experiment, the variation in *A* and g_s was significantly correlated among 11 varieties at 36, 43 and 59 DAP in 2016 ($p < 0.05$) and among 10 varieties at 43 DAP in 2017 (data not shown). These results suggest that g_s can be a determinant of the variation in leaf photosynthetic capacity among soybeans under the field condition.

Jijori and Jin dou 17 showed greater *A* and A/C_i throughout several growth stages under the field condition, while g_s of these varieties was intermediate compared with the other

varieties. It indicates that the high photosynthetic capacity of Jijori and Jin dou 17 can be achieved by the high efficiency of the gas diffusion from the intercellular spaces to the chloroplast (g_m) and/or the CO_2 fixation at the chloroplast. Peking showed high A, g_s and A/C_i among the varieties in all the measurements except for 58 DAP in 2017, indicating Peking have the high efficiency for the CO_2 supply and/or fixation.

In summary, I discovered the considerable variation in leaf photosynthetic capacity among cultivar and landrace soybeans. Three varieties, Jijori (PI 603911 C), Jin dou 17 (PI 592940) and Peking, were confirmed to exhibit the high capacity for leaf photosynthesis among soybeans under the field condition. These varieties can be utilized to enhance leaf photosynthesis by elucidating the physiological and genetic mechanisms underlying the photosynthetic capacity of them.

Table S1.1 List of line number, plant introduction (PI) number, the stem growth habit and maturity group of 34 soybean varieties.

PI no.	growth habit	maturity group
PI 360848	D-type	4
PI 398200	D-type	4
PI 398334	D-type	4
PI 398406	D-type	4
PI 398695	D-type	4
PI 398915	D-type	4
PI 399027	D-type	4
PI 399094	D-type	4
PI 404159	D-type	4
PI 407832 B	D-type	4
PI 407959 A	D-type	4
PI 408073	D-type	4
PI 408111	D-type	4
PI 408131 B	D-type	4
PI 408140 B	D-type	4
PI 408269 A	D-type	4
PI 417107	D-type	4
PI 417345 A	D-type	4
PI 423888	D-type	4
PI 424149	D-type	4
PI 424296 A	D-type	4
PI 424381	D-type	4
PI 424402 A	D-type	4
PI 424489 B	D-type	4
PI 424511	D-type	4
PI 424549 A	D-type	4
PI 442012 B	D-type	4
PI 458098	D-type	4
PI 592940	D-type	4
PI 594287	D-type	non avairable
PI 639187	D-type	4.8
PI 567174 C	D-type	4
PI 594409 A	D-type	4
PI 603911 C	D-type	4

Chapter 3

Physiological factors related to the high capacity for leaf photosynthesis in soybean

3.1 Introduction

In Chapter 2, I revealed the significant variation in leaf photosynthetic capacity among soybean varieties and identified three varieties, Jijori, Jin dou 17 and Peking, with the high photosynthetic capacity. Such variation in leaf photosynthetic capacity can be attributed to the variation in the biochemical and morphological characteristics of the leaf (Flood et al., 2011). The understanding of the physiological factors related to the high photosynthetic capacity can be important to determine the key trait for the genetic improvement of leaf photosynthetic capacity in soybean.

Leaf photosynthesis is considered as the combined process of supplying CO_2 from the atmosphere to the chloroplast and the fixation of CO_2 at the chloroplast. The gas diffusion conductance from the atmosphere to the chloroplast is divided into two components, stomatal (g_s) and mesophyll (g_m) conductance, which can limit A in plant species. (Sharkey, 1982; Pons et al., 2009). The g_s can be determined by the water status in the

leaf and the morphological characteristic such as the size and density of stomata (Flexas et al., 2004; Franks and Breeling, 2009). It is known that g_m can be largely determined by the surface area of chloroplasts exposed to intercellular spaces and the thickness of the mesophyll cell wall (Evans, 1999; Evans et al., 2009).

At the current [CO_2] of the atmosphere, the CO_2 fixation can be limited by the carboxylation of RuBP catalyzed by Rubisco. The carboxylation of RuBP can be mainly determined by the catalytic turnover rate (k_{cat}), amount and the activation state of Rubisco *in vivo*. Rubisco activase mediates the ATP-dependent removal of various inhibitory sugar phosphates from the Rubisco active site and regulates the activation of Rubisco (Portis, 1992). The N content per unit leaf area has been also demonstrated to correlate with *A* among several crop species, since large portion of N can be distributed to Rubisco in C_3 plants species (Evans, 1983; Evans, 1989; Sinclair and Horie, 1989).

In Chapter 3, I aimed to elucidate the physiological factors responsible for the great capacity for leaf photosynthesis in soybeans. To reach this objective, the biochemical and morphological traits related to the CO_2 supply and fixation in leaf photosynthesis were analyzed among the soybean varieties used in Chapter 2.

3.2 Materials and methods

3.2.1 Materials and cultivation of plants

In Chapter 3, the same soybean plants as used in the field experiments in Chapter 2 were applied for the physiological analyses mentioned below.

3.2.2 Analysis of the maximum rate of carboxylation and electron transport

The gas exchange measurements were conducted with a portable gas-exchange system (LI-6400 and LI-6800, *LI-COR*, Lincoln, NE, USA). The *A* at several [CO_2] was measured to obtain the A–C_i curves at the uppermost fully expanded leaf at 59, 67 and 71 DAP in 2014 (n = 4), at 43, 49 and 59 DAP in 2016 (n = 4–5), respectively. In 2017, the gas exchange measurements were conducted to obtain the response curve of *A* to [CO_2] at the site of Rubisco (C_c) at 46, 51and 58 DAP (n = 3–4). The [CO_2] in the chamber was set to 100, 200, 300, 400, 500, 600, 750, and 1000 ppm in 2014, while it was set to 100, 200, 300, 400 in 2016 and 2017. The light intensity was a PPFD of 2000 µmol m^{-2} s^{-1} in 2014 and 1500 µmol m^{-2} s^{-1} in 2016 and 2017, respectively. An air temperature in the chamber was set on 33°C in 2014 and 2016, and on 35°C in 2017. In 2016, the measurements were conducted with the leaves on the petioles which were cut under the water immediately before the measurements. The A–C_i and A–C_c curves were analyzed to estimate V_{cmax} and J_{max}, defined as the maximum rates of the carboxylation and

electron transport, respectively, using the biochemical model described by Farquhar et al., (1980) with some modifications by Bernacchi et al., (2001) and McMurtrie and Wang (1993) (eqn. 1 and 2);

$$A = \frac{Vc_{\max}(C - \Gamma^*)}{C + K_c(1 + O/K_o)} - R_m \quad \text{(eqn. 1)}$$

$$A = \frac{J_{\max}(C - \Gamma^*)}{4C + 8\Gamma^*} - R_m \quad \text{(eqn. 2)}$$

where C is the [CO_2], Γ^* is the CO_2 compensation point at the chloroplast, R_m is the daytime mitochondrial respiration, K_c and K_o is Michaelis-Menten constant of Rubisco for CO_2 and O_2, respectively. The values of these parameters were applied from Bernacchi et al., (2001).

3.2.3 Analysis of the mesophyll conductance using the variable *J* method

Mesophyll conductance (g_m) was estimated using the variable *J* method as described in Harley et al., (1992). Chlorophyll fluorescence measurements were simultaneously conducted with the A–C_i measurements at 46, 51 and 58 DAP in 2017. The leaf absorptance for red and blue light was set to 0.843. The relationship among A, an electron transport rate (J) and, C_c can be modeled as equation 3, according to Farquhar et al.,

(1980);

$$J = (A + R_m) \frac{4C_c + 8\Gamma^*}{C_c - \Gamma^*} \quad \text{(eqn. 3)}$$

C_c can be related to C_i as equation 4;

$$C_c = C_i - A / g_m \quad \text{(eqn. 4)}$$

Then, equation 3 can be rearranged by equation 4;

$$J = 4 (A + R_m) \frac{(C_i - A / g_m) + 2\Gamma^*}{(C_i - A / g_m) - \Gamma^*} \quad \text{(eqn. 5)}$$

R_m was estimated in two varieties, Jijori and PI 407832 B, which showed contrasting A at 43 DAP in 2017, as described by Walker et al., (2015). For the R_m estimation, A at several [CO_2] was measured to obtain the A–C_i curves at 49, 50, 55, 56, 62 and 63 DAP in 2017. The A–C_i measurements were conducted under the light intensity of 50, 80, 120, 175 and 300 µmol m^{-2} s^{-1}, respectively, with the leaves on the petioles which were cut under the water before the pre-dawn. The [CO_2] in the chamber was set to 30, 50, 70, 90, 120, 150 and 400 ppm. An air temperature in the chamber was set on 35°C. To estimate R_m for other three varieties, it was assumed that the value of R_m could be correlated with that of V_{cmax}. The Γ* was calculated based on leaf temperature using the temperature-response curve of Γ* obtained in tobacco (Bernacchi et al., 2002).

3.2.4 Quantification of the nitrogen and proteins related to leaf photosynthesis

The total soluble protein (TSP), chlorophyll, Rubisco and nitrogen (N) contents per unit leaf area were determined at the same leaf as the gas exchange measurements were conducted in 2014. A leaf tissue area of 4.52 cm^2 was collected from the leaf for the quantification of TSP, Rubisco and chlorophyll. After the area of the remaining leaf was measured, the leaf was dried at 70 °C for 72 h, weighed, and coarsely ground for N quantification. The N content per unit leaf area was determined using Kjeldahl digestion followed by an indophenol assay (Vickery et al., 1946). In 2016 and 2017, I measured the N content with the whole leaf at which the gas exchange measurements were conducted. Leaf tissues were homogenized using a cold mortar and pestle in the extraction buffer, containing 50 mM Hepes-KOH, 5mM $MgCl_2$, 1mM EDTA, 0.1% (w/v) polyvinylpolypyrrolidone (PVPP), 0.05% (v/v) Triton X-100, 5% glycerol, 4mM amino-n-caproic acid, 0.8 mM benzamidine-HCl, and 5 mM dithiothreitol (DTT) at pH 7.4, with a small amount of quartz sand. A 200 μL aliquot was set aside for the chlorophyll quantification. The homogenate was centrifuged at 14,500 × *g* for 5 min at 4°C. The supernatant was used for the quantification of TSP and Rubisco, with bovine serum albumin as the standard. The TSP content was determined by the Bradford assay

(Bradford, 1976). The Rubisco content was quantified spectrophotometrically by the formamide extraction of the bands corresponding to the large and small subunits of Rubisco separated by SDS-PAGE (Makino et al., 1986) using bovine serum albumin as the standard. The chlorophyll content extracted in 80% acetone was quantified spectrophotometrically as described by Porra et al., (1989).

3.2.5 Analysis of Rubisco activity and activation state

To determine the k_{cat} of Rubisco in soybean, a leaf tissue (2.26 cm^2) was sampled from the uppermost fully expanded leaf of UA 4805 from 09:00 to 13:00 h on 36 DAP in 2016 and frozen in liquid N. The leaf tissue was homogenized in 1 mL of extraction buffer, containing 4 mM amino-n-caproic acid, 20 mM ascorbic acid, 0.8 mM benzamidine, 100 mL Bicine-NaOH, 5 mM DTT, 1 mM EDTA, 5 mM $MgCl_2$, and 2 mM NaH_2PO_4 at pH 8.0 with 0.4% (w/v) bovine serum albumin (BSA), 1% (w/v) PVPP, and quartz sand using a tilled pestle and mortar. The homogenate was centrifuged at 12,000 rpm for 2 min at 4°C. The supernatant was used for the determination of Rubisco activity and catalytic site. The extracted Rubisco was fully activated with 15 mM $MgCl_2$ and 10 mM $NaHCO_3$ on ice for 20 min. Rubisco total activity was measured at 30°C using [^{14}C] $NaHCO_3$ by assaying the incorporation of [^{14}C] in acid-stable products with some modifications, as

described by Ishikawa et al., (2009). In the present study, 1M HCl was added to the assay solution to stop the reaction. The Rubisco catalytic site was estimated by measuring the stoichiometric binding of [^{14}C] carboxyarabinitol-1,5-bisphosphate as described by Ishikawa et al., (2009). The k_{cat} of Rubisco was calculated based on Rubisco total activity and catalytic site.

The kinetic properties of Rubisco are known to be largely determined by Rubisco large subunit (*RbcL*) (Anderson and Backlund, 2008). In the present study, genomic DNA was extracted from the leaf of Jijori, PI 594409 A, Tachinagaha and UA 4805 using DNA Prep Kit (for Plant) (*Cica Geneus*). Three partial fragments of *RbcL* were amplified by PCR using three pairs of primers; RbcL1-F GTCGAGTAGACCTTGTTGTTTCG, RbcL1-R AGCTCTACCATAATTCTTAGCGG, RbcL2-F TGCGTGCTCTACGTCTGGAG, RbcL2-R GTGAACATGATCTCCACCAG, RbcL3-F ACTAGCTTGGCTCATTATTGCC, RbcL3-R CCTTTTAGGAAAAGATTGGGCCG. PCR products were purified by FastGene Gel/PCR Extraction Kit (*NIPPON Genetics Co, Ltd*). The base sequences of three fragments were determined to assemble the full-length sequence of *RbcL*. There was no difference in the full-length sequence of *RbcL* among four soybean varieties (data not shown). In addition, Makino et al., (1987) showed the quite small variation of the k_{cat} of Rubisco among 25 varieties of rice. These facts support

the consideration that the k_{cat} of Rubisco is similar among four soybean varieties used in this study. I measured the k_{cat} of Rubisco in UA 4805 and assumed that it would be constant among soybean varieties.

To measure Rubisco initial activity, the leaf tissue (2.26 cm^2) was sampled from the uppermost fully expanded leaf of Jijori, PI 594409 A, Tachinagaha and UA 4805 after the measurements of *A* at 36 and 59 DAP and immediately frozen in liquid N. The leaf tissue was ground to a fine powder in liquid N using a pestle and mortar. The leaf powder was suspended in 125 µl of extraction buffer, containing 50 mM Bicine-NaOH, 20 mM ascorbic acid, 5 mM DTT, and 0.1 mM EDTA at pH 8.0, and subsequently centrifuged for a few seconds. The supernatant was used for the determination of Rubisco activity and catalytic site. The Rubisco total activity was calculated using the k_{cat} of Rubisco for UA 4805 and the catalytic site concentrations in each variety. The activation state of Rubisco was calculated as the percentage of Rubisco initial activity to the total activity (n = 4–5).

3.2.6 Quantification of Rubisco activase

The supernatant obtained from the Rubisco initial activity analysis was used for the quantification of TSP and Rubisco activase. In addition, TSP was extracted from the leaf

of a rice cultivar, Nipponbare, as described by Ishikawa et al., (2011). The concentration of TSP was determined in soybean and rice using the Bradford assay with BSA as the standard in 2016 (Bradford, 1976). SDS-PAGE was conducted with 6.4 µg of TSP among soybeans varieties described by Ishikawa et al., (2011). 3.2 µg of TSP extracted from rice was also applied as the standard to quantify Rubisco activase content of soybean varieties using SDS-PAGE. The gel was subjected to immunoblotting with the antibody against Rubisco activase of rice. The immunoreactive band was detected using alkaline phosphatase, as described by Fukayama et al., (2006). The relative amount of Rubisco activase was calculated in soybeans by comparing the detected bands corresponding to the large (RcaI) and small (RcaII) isoform of Rubisco activase of each soybean variety with those of rice (n = 4–5). The images were analyzed using the gel analysis tool of Image J software (Schneider et al., 2012).

3.2.7 Analysis of the morphological traits related to leaf photosynthesis

In the field experiment in 2014, the leaf anatomical structure was analyzed in a resin section prepared as follows. Leaf samples (5 mm × 5 mm) were collected from the leaf from which the A–C_i analysis were conducted on 67 and 71DAP. They were fixed in FAA solution (ethanol:water:formalin:acetic acid, 12:6:1:1 v/v). Subsequently, the leaf tissues

were dehydrated in a graduated ethanol series and the ethanol inside the leaf tissues was replaced by Technobit 7100 resin (*Heraeus Kulzer*, Wehrheim, Germany). The solidified resin including the leaf tissue was prepared following the manufacturer's protocol and cut into 5 μm sections using a motorized rotary microtome (RM2155, *Leica*, Wetzlar, Germany). The sections were colored with 0.05% toluidine blue solution for 30 min and rinsed with water for 5 min. Microscopic images were obtained with an optical microscope (CX31 and DP21, *Olympus*, Tokyo, Japan). The leaf thickness and the palisade layer thickness were measured using the image analysis software Image J.

In 2017, small leaf sections of the middle part of the uppermost fully expanded leaf were collected from three plants per each variety at 54, 55, 61 and 62 DAP. The leaf sections were infiltrated with 4% paraformaldehyde and 5 % glutaraldehyde in 0.05M Na-phosphate buffer (pH 7.2) by using Syringe pressurizer (*Nisshin EM Co., Ltd.*, Tokyo, Japan) and fixed at 4℃ for overnight. After the pre-fixation, the leaf sections were fixed in 1% OsO4 in 0.1M phosphate buffer at 4℃ for overnight. The fixed leaf sections were embedded in Epoxy Resin. An ultra-thin section was observed using transmission electron microscopes (H-7650, *Hitachi*, Tokyo, Japan) and the microscopic images were obtained. The microscopic images were analyzed to measure the thickness of the mesophyll cell wall (T_{cw}).

The stomatal density (*SD*), the number of the stomata per unit leaf area and the vein density (*VLA*), the vein length per unit leaf area, were measured at the same leaf as *A* were measured in 2016. A replica of the abaxial side of the leaf was prepared using Suzuki's Universal Method of Printing (Tanaka et al., 2010). The replica was observed at a 100× magnification using an optical microscope, and a digital image was obtained (CX31 and DP21, Olympus, Tokyo, Japan). The number of stomata in the image was manually counted to measure the *SD*. The *VLA* was measured as described in Yoshimura and Kubota (2000).

3.2.8 Statistical analysis

One-way ANOVA or the Tukey-Kramer test were applied to evaluate the variation in the physiological traits among the varieties. Statistical analyses were conducted using R.

3.3 Results

3.3.1 Variations in the maximum carboxylation rate, the maximum electron transport rate and the mesophyll conductance among soybeans

The *A*-C_i curve analysis showed that Jijori exhibited highest *A* under all the CO_2 concentrations among the four varieties except for 59 DAP in 2014. The Vc_{max} and J_{max}

of Jijori were highest of the four varieties at all the stages. There was the significant variation in Vc_{max} among the four varieties and the maximum value of these parameters were 129.1 µmol m^{-2} s^{-1} and 232.0 µmol m^{-2} s^{-1}, respectively, at 67 DAP ($p < 0.01$) (Fig. 3.1). In 2016, there was the significant variation in Vc_{max} among the 11 varieties at all the stages ($p < 0.01$). The Vc_{max} of Jijori was highest at 43 and 49 DAP and second highest at 59 DAP (Fig. 3.2). The Vc_{max} of Peking was second highest and highest of the 11 varieties at 49 and 59 DAP, respectively, while it was third lowest at 43 DAP in 2016. The Vc_{max} of Jijori and Peking was higher maximumly by 41.9 and 26.0% than the reference variety, UA 4805 at 49 DAP in 2016.

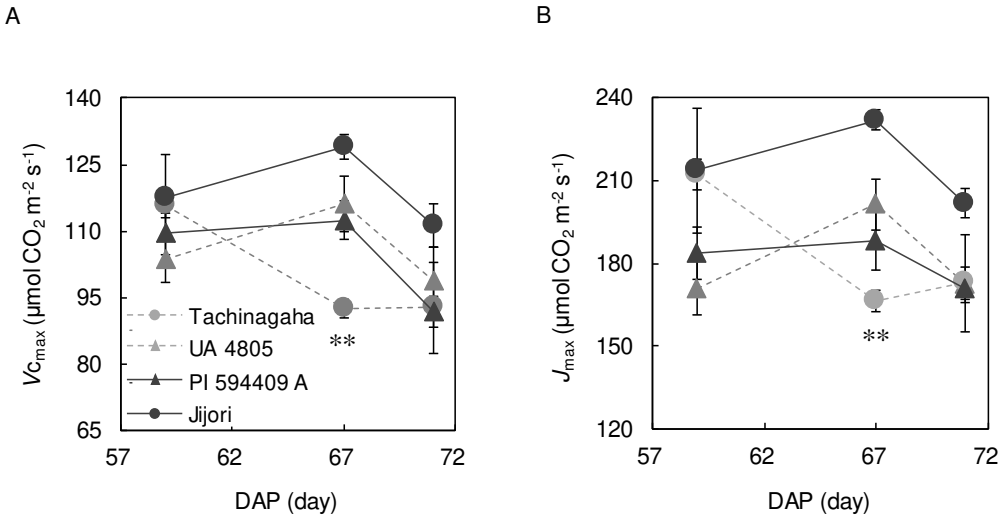

Fig. 3.1 Variations in the maximum rate of (A) the carboxylation (Vc_{max}) and (B) electron transport rate (J_{max}) among four soybean varieties in 2014.
** indicates the significant difference among four soybean varieties at $p < 0.01$. Vertical bars on symbols indicate SE (n = 4).

The Vc_{max} based on the A–C_i analysis reflects not only the maximum rate of the

carboxylation at the chloroplast but also g_m since the biochemical model described by Farquhar et al., (1980) assumes that C_i is equal to C_c (i. e. g_m can be infinite). In 2017, I estimated Vc_{max} based on the response curve of A to C_c which was estimated by substituting measured g_m for eqn. 4. There was the significant variation in Vc_{max} among the five varieties at 51 and 58 DAP ($p < 0.05$), whereas there was no significant variation at 46 DAP in 2017 (Fig. 3.3). The Vc_{max} of Jijori was highest of all the varieties at 46 and 51 DAP, while that was second lowest at 58 DAP. There was no clear difference in Vc_{max} between Enrei and Jijori at all the measurements. The Vc_{max} of Jin dou 17 and Peking was lowest or second lowest at all the stages except for that of Peking at 58 DAP. There was

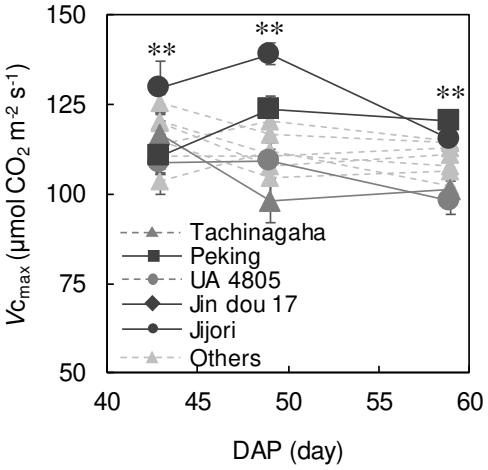

Fig. 3.2 Variation in Vc_{max} among 11 soybean varieties in 2016.

** indicate the significant difference among 11 soybean varieties at $p < 0.01$. Vertical bars on symbols indicate SE (n = 3–5).

the significant variation in g_m among five varieties at all the stages ($p < 0.01$). The g_m of Jijori, Jin dou 17 and Peking was highest, second highest and third highest, respectively, among the five varieties at all the stages. The g_m of Jin dou 17 was extremely high at 51

and 58 DAP compared with that of the other varieties and that shown among soybean varieties in the previous studies (Koester et al., 2016; Tomeo et al., 2017).

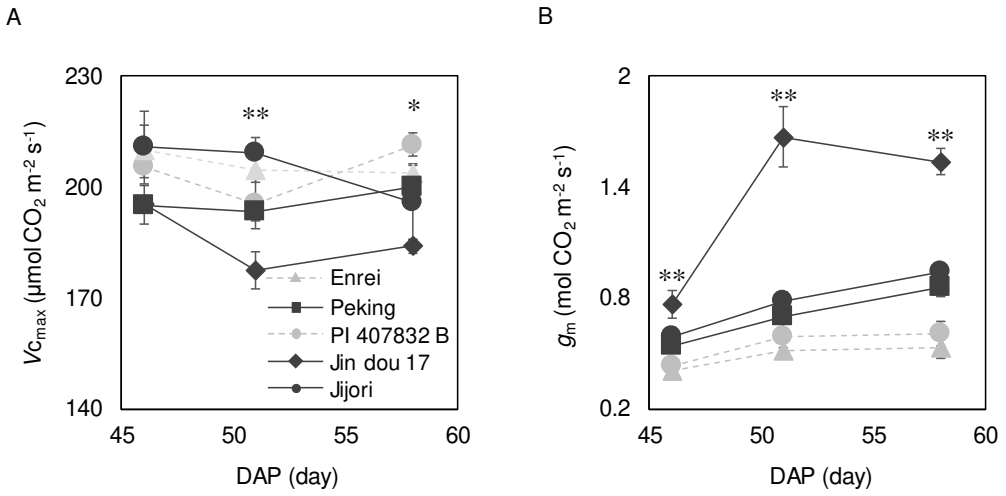

Fig. 3.3 Variations in (A) Vc_{max} and (B) the mesophyll conductance (g_m) among five soybean varieties in 2017.

* and ** indicate the significant variation among five soybean varieties at $p < 0.05$ and 0.01, respectively. Vertical bars on symbols indicate SE (n = 3–4).

3.3.2 Variations in the biochemical characteristics of the leaf among soybeans

In 2014, the TSP, chlorophyll, Rubisco, and N contents were determined with the same leaf from which leaf gas exchange was measured. The levels of these components drastically increased around R5 but it was relatively stable during the other stages in all the four varieties (Fig. 3.4). The content of these components in Jijori was highest or second highest among the four varieties at all the stages. The variation in the content of TSP and chlorophyll was not clear between Jijori and Tachinagaha which showed the

contrasting *A* as shown in Chapter 2 (Fig. 2.2). The ratio of Rubisco to TSP (Rubisco/TSP) of Jijori was highest or second highest among the four varieties at all the stages (Fig. 3.5).

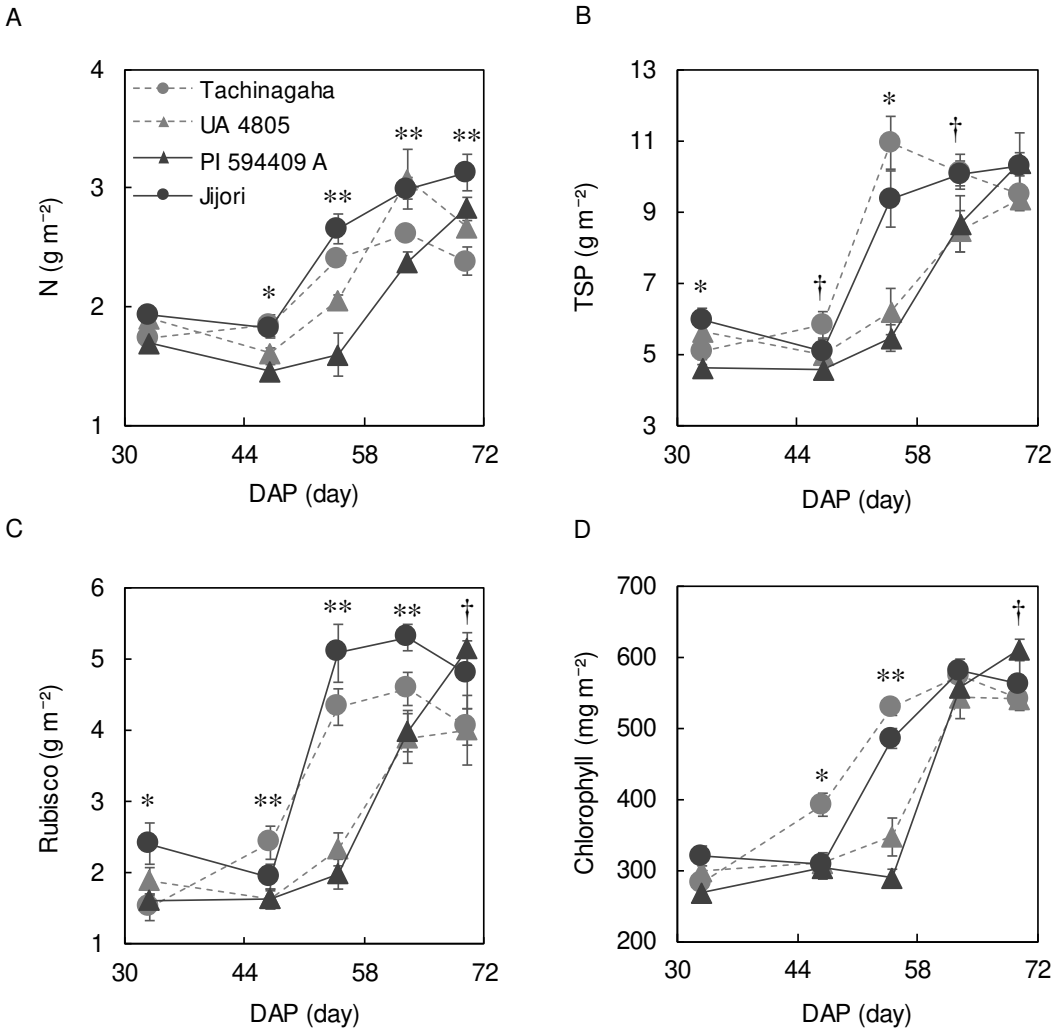

Fig. 3.4 Variations in the content of (A) nitrogen (N), (B) total soluble protein (TSP), (C) Rubisco and (D) chlorophyll among four soybean varieties in 2014. †, * and ** indicate the significant variation among four soybean varieties at $p < 0.1$, 0.05 and 0.01, respectively. Vertical bars on symbols indicate SE (n = 8–10).

In 2016 and 2017, there was the significant variation in the N content among the 11 and five varieties, respectively, except for 43 DAP in 2016 ($p < 0.05$) (Fig. 3.6). The N

content of Jijori was tended to be higher than the others at 49 and 59 DAP, while that was intermediate at 36 and 43 DAP in 2016. The N content of Peking was second highest

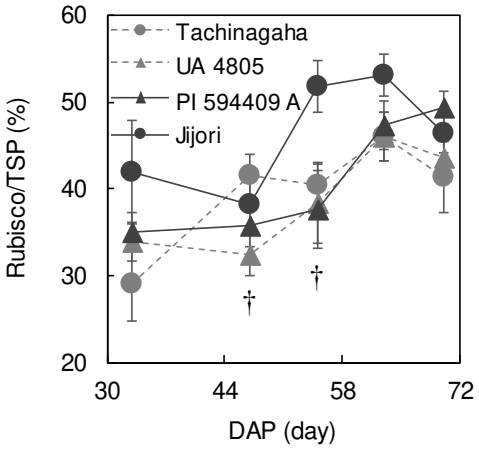

Fig. 3.5 Variation in the ratio of Rubisco to TSP (Rubisco/TSP) among four soybean varieties in 2014.

† indicates the significant variation among four soybean varieties at $p < 0.1$. Vertical bars on symbols indicate SE (n = 8–10).

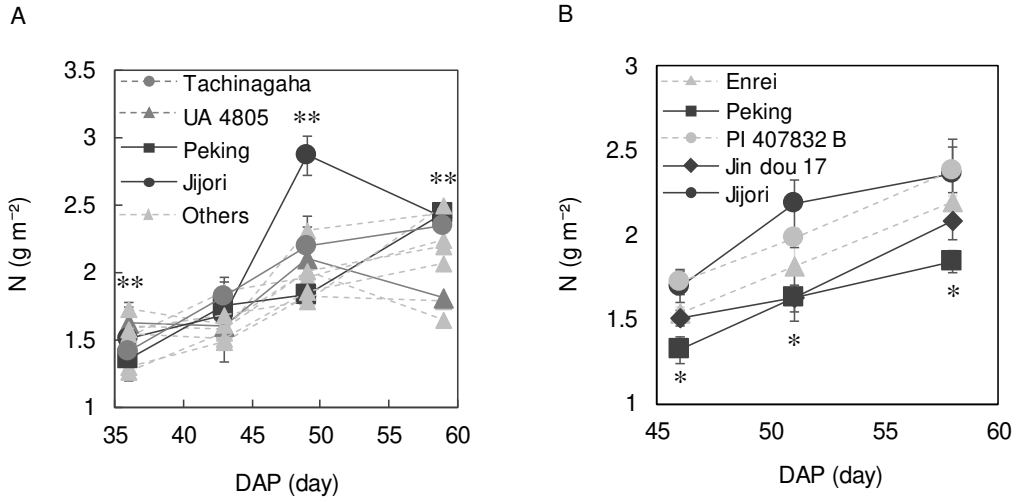

Fig. 3.6 Variation in the N content among soybeans in (A) 2016 and (B) 2017.

* and ** indicate the significant variation among the soybean varieties at $p < 0.05$ and 0.01, respectively. Vertical bars on symbols indicate SE (n = 3–6).

among 11 varieties at 59 DAP, while that was intermediate or lower among the varieties at the other stages. In 2017, the N content of Jijori was highest or second highest among five varieties at all the stages, while that of Jin dou 17 and Peking lowest or second lowest.

In 2016, the N content ranged from 1.55 to 1.79 g m^{-2} at 36 DAP, and from 2.14 to 2.39 g m^{-2} at 59 DAP among Jijori, PI 594409 A, Tachinagaha and UA 4805 (Fig. 3.7). The N content significantly increased from 36 to 59 DAP in all the varieties (p<0.05). The catalytic turnover rate (k_{cat}) of Rubisco was 2.62 mol mol^{-1} s^{-1} in UA 4805 at 36 DAP. In the present study, this value of k_{cat} was used for the calculation of the activation state of Rubisco in each variety. The activation state of Rubisco varied from 62.9 to 82.9% at 36 DAP, and from 55.3 to 60.0% at 59 DAP. The activation state of Rubisco significantly decreased from 36 to 59 DAP in Jijori, Tachinagaha and UA 4805 (p<0.01). The ratio of Rubisco to TSP ranged from 0.47 to 0.57 g g^{-1} at 36 DAP, and was the similar level at 59 DAP among the four varieties in 2016. The ratio of Rubisco to TSP significantly decreased from 36 to 59 DAP in Jijori, PI 594409 A and UA 4805, whereas it was largely constant in Tachinagaha (p<0.01). When standardized by the TSP amount, the relative amount of Rubisco activase ranged from 0.90 to 1.09 at 36 DAP, and from 0.49 to 0.95 at 59 DAP. The Rubisco activase amount was largely constant from 36 to 59 DAP in Jijori, PI 594409 A and UA 4805, whereas it significantly decreased in Tachinagaha (p < 0.01).

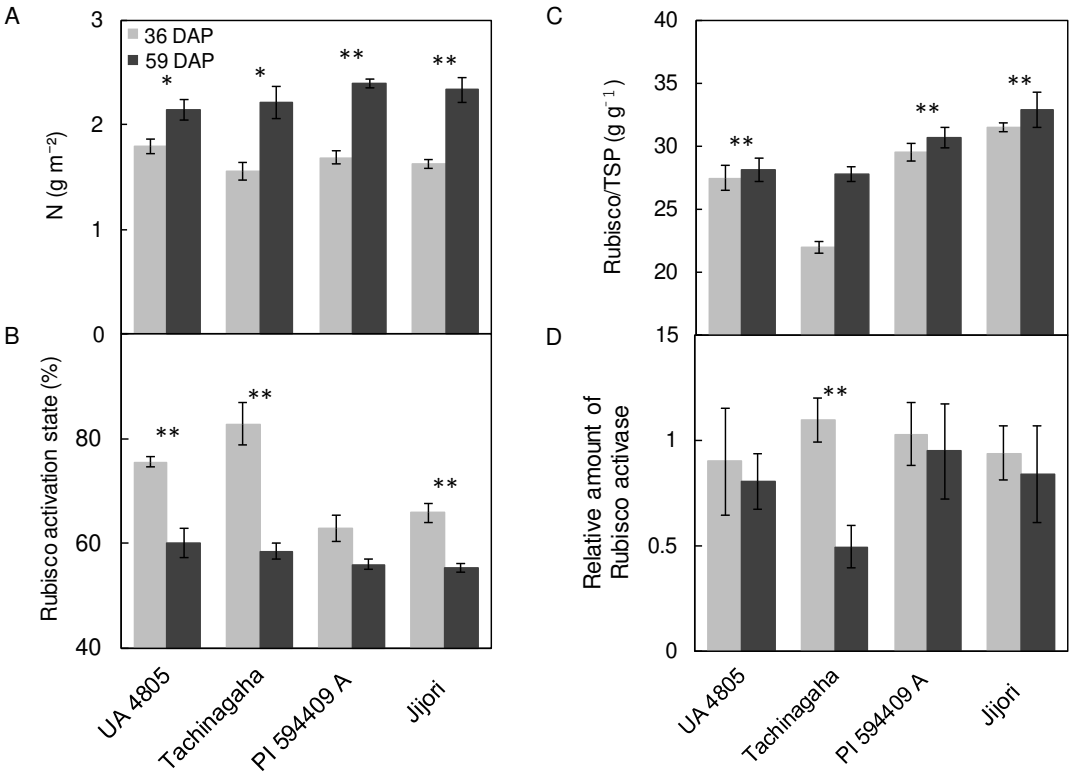

Fig. 3.7 Changes in (A) the N content, (B) Rubisco activation state, (C) Rubisco/TSP and relative amount of Rubisco activase of four soybean varieties in 2016.

* and ** indicate the significant variation between the values of the traits in each variety at 36 and 59 DAP at $p < 0.05$ and 0.01, respectively. Vertical bars on symbols indicate SE (n = 4–6).

3.3.3 Variations in the morphological characteristics of the leaf among soybeans

In 2014, the leaf structure was analyzed in the same leaf from which the A–C_i curves were obtained on 67 and 71 DAP. Leaf thickness of Jijori was significantly higher than that of the others at 67 DAP ($p < 0.05$) (Table 3.1). The palisade layer thickness of Jijori was significantly higher than that of PI 594409 A and UA 4805 at 67 DAP, and UA 4805 at 71 DAP, respectively ($p < 0.05$). There was a significant variation in the ratio of the

palisade layer thickness to the leaf thickness (palisade/leaf ratio) between Jijori and UA 4805 at 67 DAP ($p < 0.05$). The palisade/leaf ratio of all the varieties was stable across the two measurements.

In 2016, there was the significant variation in *SD* at 49 and 59 DAP among the 11 varieties ($p < 0.01$) (Fig. 3.8). There was the significant variation in *VLA* at all the stages ($p < 0.05$). The *SD* and VLA of Jijori were lowest or second lowest among the 11 varieties at all the stages, while those of Peking were intermediate. The *VLA* of the reference variety, UA 4805, was highest at all the stages.

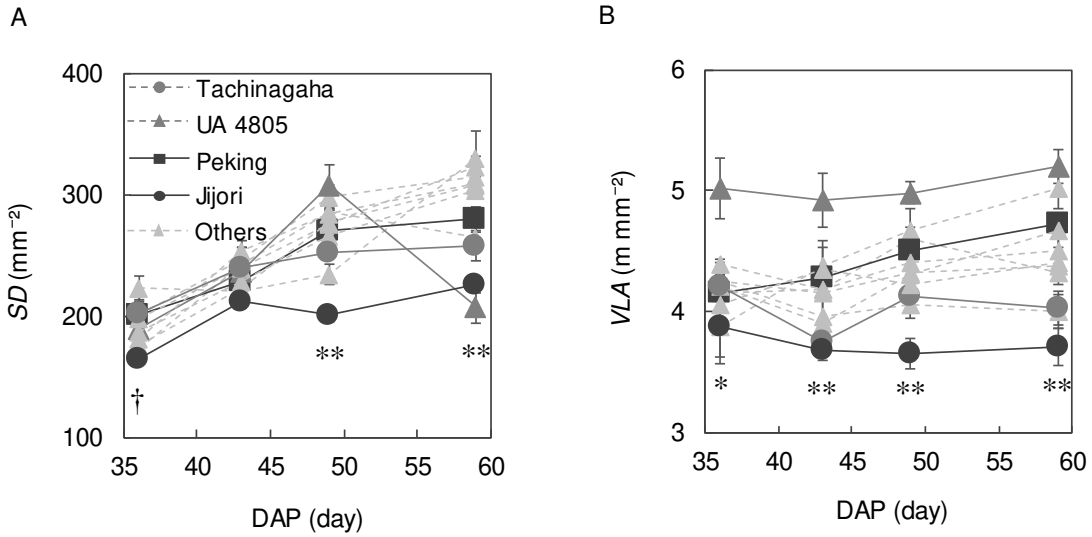

Fig. 3.8 Variations in (A) the stomatal density (*SD*) and (B) the vein density (*VLA*) among the 11 soybean varieties in 2016.
†, * and ** indicate the significant variation among 11 soybean varieties at $p < 0.1$, 0.05 and 0.01, respectively. Vertical bars on symbols indicate SE (n = 4–6).

In 2017, T_{cw} was measured at the uppermost fully expanded leaves among five

varieties in which the g_m measurements were conducted. There was the significant variation in T_{cw} among four varieties except for Enrei at both stages ($p < 0.05$) (Fig. 3.9). The T_{cw} of Jin dou 17 was lowest among the varieties at 54 DAP. There was the significant variation between Jin dou 17 and Jijori or PI 407832 B at this stage. At 61 DAP, T_{cw} of Enrei was lowest, although the replication number was only two. The T_{cw} of Jin dou 17 and Peking were significantly lower than Jijori at 61 DAP.

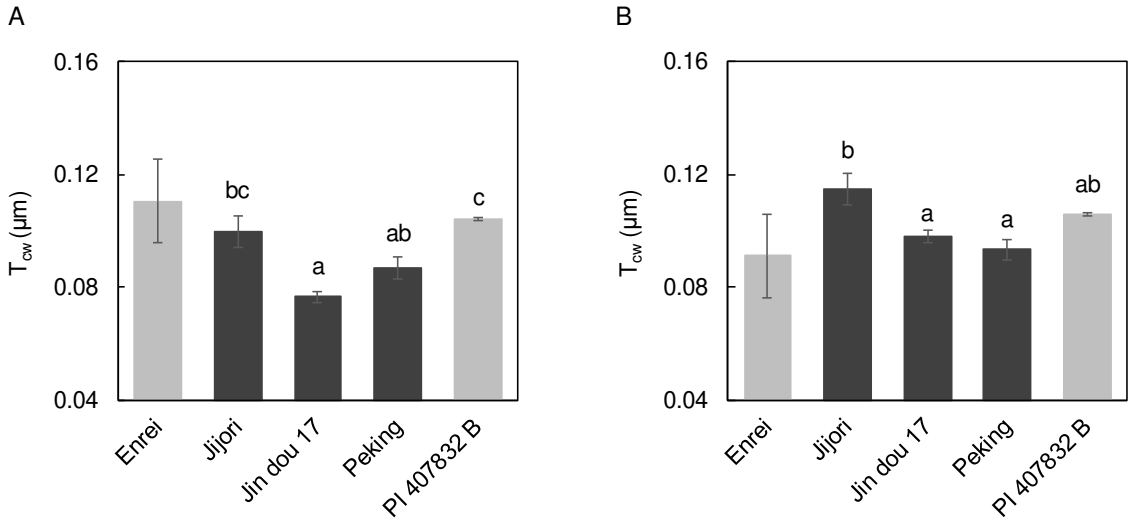

Fig. 3.9 Variation in the thickness of the mesophyll cell wall (T_{cw}) among five soybean varieties in 2017.
Different letters on each column indicate the significant variation at $p < 0.05$. Vertical bars on columns indicate SE (n = 2–3).

3.4 Discussion

In Chapter 3, I aimed to elucidate the physiological factors responsible for the high capacity for leaf photosynthesis in three varieties, Jijori, Jin dou17 and Peking. To reach

this objective, the efficiencies of the CO_2 diffusion inside the leaf and the CO_2 fixation at the chloroplast were analyzed based on the gas exchange measurements. In addition, the biochemical and morphological traits related to leaf photosynthesis were analyzed.

The A–C_i analysis in all the years revealed high A of Jijori, Jin dou 17 and Peking at any C_i among soybeans. It suggests that these varieties can have the high efficiency of the CO_2 diffusion inside the leaf and/or the CO_2 fixation at the chloroplast. In 2017, g_m of these varieties was significantly higher than Enrei and PI 407832 B (Fig. 3.3) and the variation in g_m and A was consistent among the five varieties. Jin dou 17 showed the extremely high value of g_m at 51 and 58 DAP, compared with that of the other varieties and that reported in the previous studies (Koester et al., 2016; Tomeo et al., 2017), indicating the possibility that g_m of Jin dou 17 might be overestimated due to some problems for these measurement. On the other hand, Jin dou 17 showed comparable A with Jijori, while g_s and the N content per unit leaf area were similar or lower (Figs. 2.5, 3.6), which would evidence high g_m of Jin dou 17 among soybeans.

It was shown that g_m was correlated with the surface area of chloroplasts exposed to intercellular spaces (Evans, 1999). The T_{cw} is known to have the large resistance for CO_2 diffusion, accounting for up to 50% of total resistance (Evans et al., 2009). In addition, the permeability of CO_2 via plasma membrane and chloroplast envelope can be a major

Table 3.1 Leaf thickness, palisade layer thickness, and ratio of the palisade layer thickness to the leaf thickness (Plisade / leaf) of four soybean varieties in 2014.

	67 DAP				71 DAP			
	UA 4805	Tachinagaha	PI 594409 A	Jijori	UA 4805	Tachinagaha	PI 594409 A	Jijori
Leaf thickness, µm	194.5 bc	204.6 b	164.4 c	248.0 a	188.7 a	226.7 a	197.5 a	235.9 a
Palisade layer thickness, µm	102.7 bc	125.9 ab	95.5 c	150.5 a	101.8 b	132.1 ab	116.5 ab	141.5 a
Palisade / leaf	0.53 b	0.62 a	0.58 ab	0.61 a	0.54 a	0.58 a	0.59 a	0.60 a

component of the resistance. In the present study, the variation in T_{cw} and g_m among five varieties was consistent at 54 DAP, while that was not consistent at 61 DAP (Figs. 3.3 and 3.9). It suggests that T_{cw} can have a large effect on g_m in soybean at the specific growth stage.

The potential of g_s can be mainly determined by the morphological characteristics of the stomata (Franks and Breeling, 2009). In soybean, *SD* was reported to strongly correlate with the potential of g_s among 77 cultivars (Tanaka et al., 2010). Moreover, g_s can be largely affected by the water status in the plant (Flexas et al., 2004). The leaf hydraulic conductance, representing the efficiency of water transpiration inside the leaf, was reported to correlate with *A* and g_s among or within species (Brodribb et al., 2007; Xiong et al., 2015). The *VLA* can be correlated with hydraulic conductance since *VLA* can determine the parallel pathways of water flow through the vein system per unit leaf area and the distance of water flow from veins to the sites of evaporation. In the present study, Peking showed high g_s throughout the years and stages among soybeans, which can contribute to high *A* in this variety (Fig. 2.5). On the other hand, *SD* and *VLA* of Peking was intermediate among 11 varieties at all the stages in 2016 (Fig. 3.8). These results suggest that high g_s of Peking can be attributed to unknown factors rather than *SD* and *VLA*.

The N content per unit leaf area is one of the most important traits determining leaf photosynthetic capacity because a large portion of leaf N is allocated to the photosynthetic components, especially to Rubisco (Hikosaka, 2010). The amount and kinetic properties of Rubisco limit CO_2 fixation activity. It has been reported that the Rubisco content and its activity determined the changes in leaf photosynthetic capacity in the course of senescence under field conditions in soybean (Jiang et al., 1993). In the present study, Vc_{max} based on A–C_c analysis was tended to be higher in Jijori among the five varieties, while that was lower in Jin dou 17 and Peking. The N and Rubisco content of Jijori tended to be higher than in the other varieties (Figs. 3.4 and 3.6). The leaf of Jijori was thicker than the leaves of the other genotypes (Table 3.1). It has been reported that leaf photosynthetic capacity is correlated with leaf thickness and N content in soybean (Ojima, 1972). These results imply that a thicker leaf can accumulate a large amount of N and photosynthetic apparatus, especially Rubisco, and have an advantage in achieving high photosynthetic capacity due to the high CO_2 fixation activity. The ratio of TSP to N of Jijori was similar to or lower than that of the other varieties, while the Rubisco/TSP in Jijori was higher than that of the other genotypes (Fig. 3.5). This shows that the large amount of Rubisco of Jijori can be attributed to the large distribution of TSP to Rubisco. Kawasaki et al., (2014) reported that there was considerable variation in the ratio of

Rubisco to N in soybean under field conditions. Thus, protein distribution in the leaf can also be a target to select soybean varieties with high photosynthetic capacity.

In 2016, A and A/C_i were largely constant from 36 to 59 DAP in Jijori, PI 594409 A and UA 4805, whereas the N content significantly increased in all the varieties (Figs. 2.3 and 3.6). The activation state of Rubisco significantly decreased during this period in Jijori, Tachinagaha, UA 4805 ($p<0.01$) (Fig. 3.7). These results showed that the activation state of Rubisco can decrease with the increase in the N content, which can result in the constant A during the reproductive stage of soybean. A negative correlation between the activation state of Rubisco and the N content was observed in wheat and apple with various N application levels (Mächler et al., 1988; Chen and Fuchigami, 2000). The present study shows that the deactivation of Rubisco with the N accumulation can be observed even across different growth stages in soybean with the same N application level.

In the transgenic tobacco, the decrease in Rubisco activase content resulted in the deactivation of Rubisco (Mate et al., 1993; Jiang et al., 1994). In the present study, the Rubisco/TSP significantly decreased from 36 to 59 DAP, whereas the relative amount of Rubisco activase was largely constant in Jijori, PI 594409 A and UA 4805 (Fig. 3.7). This suggests that the decrease in the activation state of Rubisco was attributed to an unknown mechanism other than to the deficiency of Rubisco activase per Rubisco amount in these

three genotypes. Perdomo et al., (2017) suggests that the decrease in the activation state of Rubisco can be related to not Rubisco activase amount but its activity under high temperature and water deficit condition in crop plants. In the present study, the deactivation of Rubisco might be associated with the decrease in the activity of Rubisco activase. In Tachinagaha, on the other hand, the Rubisco/TSP was largely constant during this period, whereas the relative amount of Rubisco activase decreased to approximately one-half. The decrease in the activation state of Rubisco in Tachinagaha might be attributed to the deficiency of Rubisco activase per Rubisco amount.

In 2014, I showed the drastic increase in the Rubisco content with the increase in the N content throughout the reproductive stage of the four soybean varieties. Based on the observation of the N content, the increase in the Rubisco content was expected among four varieties, although the Rubisco content was not measured in 2016 and 2017. It was suggested that the change in the Rubisco content affected the wide range of metabolites in Calvin cycle and the energy status in chloroplasts (Suzuki et al., 2012). The carbamylation state of Rubisco is affected by the activity of Rubisco activase. The activity of Rubisco activase is found to be sensitive to ATP/ADP ratio, since Rubisco activase requires ATP for its function and is inhibited by ADP (Portis et al., 1992). The activation state of Rubisco increased with the increase in ATP/ADP ratio in transgenic tobacco with

decreased Rubisco content (Quick et al., 1991). The activity of Rubisco activase can be also affected by its redox change mediated by ferredoxin-thioredoxin, which can alter the sensitivity of Rubisco activase to the inhibition by ADP (Zhang et al., 2002). In addition, the activation state of Rubisco can be affected by stromal pH and metabolites such as RuBP and phosphoglyceric acid (Servaites, 1991; Portis et al., 2003). Overall, the deactivation of Rubisco observed in the present study might result from the above change in the Calvin cycle metabolites and energy status with increasing the Rubisco content in soybean.

In summary, I revealed greater mesophyll conductance (g_m) in Jijori, Jin dou 17 and Peking, which showed greater *A* among soybeans. In addition, Jijori and Peking showed the additional advantage in the different physiological traits, V_{cmax} and g_s, respectively. Jijori showed the high N and Rubisco content per unit leaf area, which could contribute to the high CO_2 fixation activity in this variety. These results suggest that there can be several traits as the target to enhance leaf photosynthetic capacity in soybean and simultaneous improvement of these trait has the potential to achieve the drastic enhancement of leaf photosynthetic capacity.

Chapter 4

Genetic factors related to the high capacity for leaf photosynthesis in soybean.

4.1 Introduction

In Chapter 2, I revealed the significant variation in leaf photosynthetic capacity among soybeans. This variation can be determined by the genetic and environmental factors via the effect on the physiological traits related to leaf photosynthesis (Flood et al., 2011). Previous studies have reported the genetic and physiological factors responsible for the significant variation in *A* among rice cultivars (Teng et al., 2004; Hu et al., 2009; Adachi et al., 2011*a*; Adachi et al., 2011*b*). Notably, *NAL1* and *CAR8* were identified as the causal genes for such variation in rice (Takai et al., 2013; Adachi et al., 2017). In soybean, significant variation in *A* has also been observed among different varieties (Ojima, 1972; Butterry et al., 1977; Tanaka et al., 2010; Liu et al., 2012; Koester et al, 2016; Tomeo et al., 2017). The genetic factors controlling the variation in *A*, on the other hand, has remained unclear in field-grown soybeans, although a few studies have reported the genetic factors in pot-grown soybeans (Vieira et al., 2006; Yin et al., 2010; Li et al., 2016). The elucidation of the genetic factors controlling leaf photosynthesis of field-grown

soybeans can provide a novel strategy to exploit with soybean breeding.

Quantitative trait loci (QTL) analysis has been conducted in large-scale studies to identify the chromosomal regions which control the important agronomical traits in crops (Yano, 2001). The chromosome segment substitution lines (CSSLs) have been developed in rice and soybean and have accelerated QTL analyses associated with several traits of interest (Bian et al., 2010; Wang et al., 2013; Takai et al., 2014; Xin et al., 2016; Watanabe et al., 2018). Watanabe et al., (2018) developed CSSLs in soybean using the progeny of a cross between Enrei, a leading variety in Japan, and Peking, a landrace from China. In Chapter 2, greater *A* in Peking than in Enrei was found after the flowering stage under field conditions. Therefore, it is expected that the genetic analysis using the CSSLs derived from these two soybeans can identify the QTLs responsible for the high capacity for leaf photosynthesis in the Peking variety.

In Chapter 4, I aimed to elucidate the genetic factors affecting the variation in leaf photosynthetic capacity among soybeans. To reach this objective, I conducted field experiments over three years, using Enrei, Peking and the CSSLs derived from their progenies. The gas exchange measurements were conducted to evaluate *A* among soybean lines while the genetic analysis was performed to detect the QTLs responsible for the variation in *A* between Enrei and Peking. The biochemical and morphological traits

related to leaf photosynthesis were also analyzed to reveal the physiological impact of the QTL effect on leaf photosynthesis.

4.2 Materials and methods

4.2.1 Cultivation of the soybean plants in the field experiment

The present study was conducted at the Experimental Field of the Graduate School of Agriculture, Kyoto University, Kyoto, Japan (35°2′N, 135°47′E, 65 m altitude, and Fluvic Endoaquept soil type) in 2016, 2017 and 2018. The sowing date was 4 July in 2016, 27 June in 2017, and 26 June in 2018, respectively. The spacing between rows and plants was 0.7 and 0.15 m, respectively. The N, P_2O_5, and K_2O fertilizers were applied at 3, 10, and 10 g m^{-2}, respectively, before planting. In 2016 and 2017, two experimental plots were established for each soybean line, and each plot was composed of eight plants in a single row. In 2018, three experimental plots were established for each line, and each plot was composed of 40 plants in four rows. These plots were arranged in a randomized complete block design. The experimental field was frequently irrigated to avoid the negative effect of drought stress on the plant growth and gas exchange measurements. I recorded DAP when each soybean line reached R1 and R5.

4.2.2 Plant materials

In the present study, I used the Enrei and Peking varieties of soybean and 103 CSSLs derived from their progenies, which were developed by Watanabe et al. (2018). Both of the two parental lines belong to the maturity group IV. The stem growth habit is the determinate type in Enrei and the semi-indeterminate type in Peking, respectively. Each of the CSSLs carry the targeted chromosomal segment from Peking in the genetic background of Enrei. Besides the targeted segment, a few residual segments from Peking randomly remained in each CSSL. I used two parental lines in the field experiment in 2016, 2017, and 2018, respectively, and all the 103 CSSLs only in 2016.

I cultivated two types of the BC_3F_3 populations in 2017 derived from the cross between Enrei and Peking with Enrei as the recurrent parent. Chromosomal segments from 26.5 to 32.9 Mbp on chromosome 13 or from 39.9 to 42.7 Mbp on chromosome 20 were segregated in each BC_3F_3 population, respectively. These segments were located on the QTLs, *qLPC13* and *qLPC20*, respectively, from which a significant effect on *A* was shown in 2016. Total DNA of the BC_3F_3 plants was extracted from the frozen and dried leaves by the cetyltrimethylammonium bromide (CTAB) protocol (Kurata et al., 1994). In each BC_3F_3 population, the genotype of *qLPC13* or *qLPC20* was analyzed by using five and two SSR markers (Table 4S.1), respectively, reported in Watanabe et al., (2018).

From each BC_3F_3 population, I obtained two BC_3F_4 lines, which were homozygous for either the Enrei allele (E-allele) or the Peking allele (P-allele) at the targeted region, while the genetic background was mostly the same. Overall, the four BC_3F_4 lines were used with two parental lines in the field experiment in 2018.

4.2.3 Gas exchange measurements

The characteristics of leaf photosynthesis were evaluated in the soybean lines using a portable gas-exchange system LI-6400 (*LI-COR*, Lincoln, NE, USA). The gas exchange measurements were conducted at two growth stages (Stage 1 and Stage 2) after flowering. The A, g_s, and C_i were measured at the uppermost fully expanded leaf from 8:30 to 14:00 on the sunny day in conditions with a [CO_2] of 400 ppm, PPFD of 1500 μmol m^{-2} s^{-1}, and air temperature of 33 °C. The mesophyll activity was evaluated as A/C_i. The gas exchange measurements were conducted at 39, 40, 52 and 53 DAP in 2016, at 38 and 50 DAP in 2017, and at 37 and 49 DAP in 2018, respectively. In 2016, the measurements were completed in all the 105 soybean lines for two days at both Stage 1 (39 and 40 DAP) and Stage 2 (52 and 53 DAP). The measurement replication for each line was 5–6 in 2016, 4–6 in 2017 and 8–9 in 2018.

4.2.4 Analysis of the biochemical and morphological traits related to leaf photosynthesis

The N, Rubisco, and chlorophyll content per unit leaf area was measured on the same leaf as the gas exchange measurements in 2018. Leaf tissue of 1.13 cm^2 was collected from the leaf for the quantification of Rubisco and chlorophyll. After the area of the remaining leaf was measured, the leaf was dried at 70 °C for 72 h, weighed, and coarsely ground for N quantification. The N content per unit leaf area was determined using Kjeldahl digestion followed by an indophenol assay (Vickery et al. 1946). Rubisco and chlorophyll were extracted from the leaf tissue following the method described by Sakoda et al., (2016). The content of Rubisco was quantified spectrophotometrically by the formamide extraction of the bands corresponding to the large and small subunits of Rubisco separated by SDS-PAGE (Makino et al., 1986) using bovine serum albumin as the standard protein. The content of chlorophyll extracted in 80% acetone was quantified spectrophotometrically as described by Porra et al. (1989).

Stomatal density (*SD*) was also measured on the same leaf as the above analyses were conducted. A replica of the abaxial side of the leaf was prepared using Suzuki's Universal Method of Printing (Tanaka et al., 2010). The replica was observed at a 100× magnification using an optical microscope, and a digital image was obtained (CX31 and

DP21, Olympus, Tokyo, Japan). The number of stomata in the image was manually counted to measure *SD*.

4.2.5 Genetic and statistical analysis

The variation in *A* was evaluated among Enrei, Peking, and the 103 CSSLs in 2016 by a Tukey-Kramer test to detect the QTLs with the significant effect on *A*. To avoid a false negative of a QTL with small effect on *A*, I also conducted a one-way ANOVA to evaluate the variation in *A* based on the genotype of each of the 221 SSR markers designed to cover the whole chromosomal region of soybean. The flanking region of the SSR markers, in which the significant variation was detected by one-way ANOVA, were considered as the candidate QTL. In 2018, I compared the *A*, g_s and A/C_i between two BC_3F_4 lines with the Enrei allele (E-allele) or the Peking allele (P-allele) at *qLPC13* and those at *qLPC20*, respectively, by one-way ANOVA to confirm two candidate QTLs. Statistical analysis was performed using R software version 3. 5. 0 (R Foundation for Statistical Computing, Vienna, Austria).

4.3 Results

4.3.1 Characteristics of leaf photosynthesis among soybean lines

The R1 date of Enrei was two days later than that of Peking in 2016, while that of Enrei was one and five days earlier in 2017 and 2018, respectively (Table 4S.2). The R5 date of Enrei was 4—7 days earlier than that of Peking in all three years. Throughout all the stages and years, Peking showed higher A by 5.7–12.1% than that of Enrei, except for Stage 2 in 2018 ($p < 0.05$) (Figs. 4.1, 4S.1 and 4S.2). The g_s and A/C_i of Peking tended to be higher than those of Enrei, although the variation in these parameters between the two parental lines was unstable across the stages and years.

As for the 103 CSSLs, the variation in A, g_s and A/C_i was investigated in 2016. The A varied from 22.9 to 32.9 μmol m^{-2} s^{-1} at Stage 1, and from 21.7 to 33.7 μmol m^{-2} s^{-1} at Stage 2 among the 103 CSSLs (Figs. 4.2A and 4.2B). The g_s varied from 0.60 to 1.56 mol m^{-2} s^{-1} at Stage 1, and from 0.51 to 1.60 mol m^{-2} s^{-1} at Stage 2 (Fig. 4S.3). The A/C_i varied from 0.079 to 0.112 μmol m^{-2} s^{-1} ppm^{-1} at Stage 1, and from 0.076 to 0.116 μmol m^{-2} s^{-1} ppm^{-1} at Stage 2. Peking showed the highest or second highest values for these parameters compared to that of all the 105 lines at both growth stages in 2016.

4.3.2 Quantitative trait loci related to leaf photosynthesis

According to the Tukey-Kramer test, no CSSLs showed significantly higher A than Enrei at both growth stages in 2016. On the other hand, three CSSLs, B0446, B0920, and B0950,

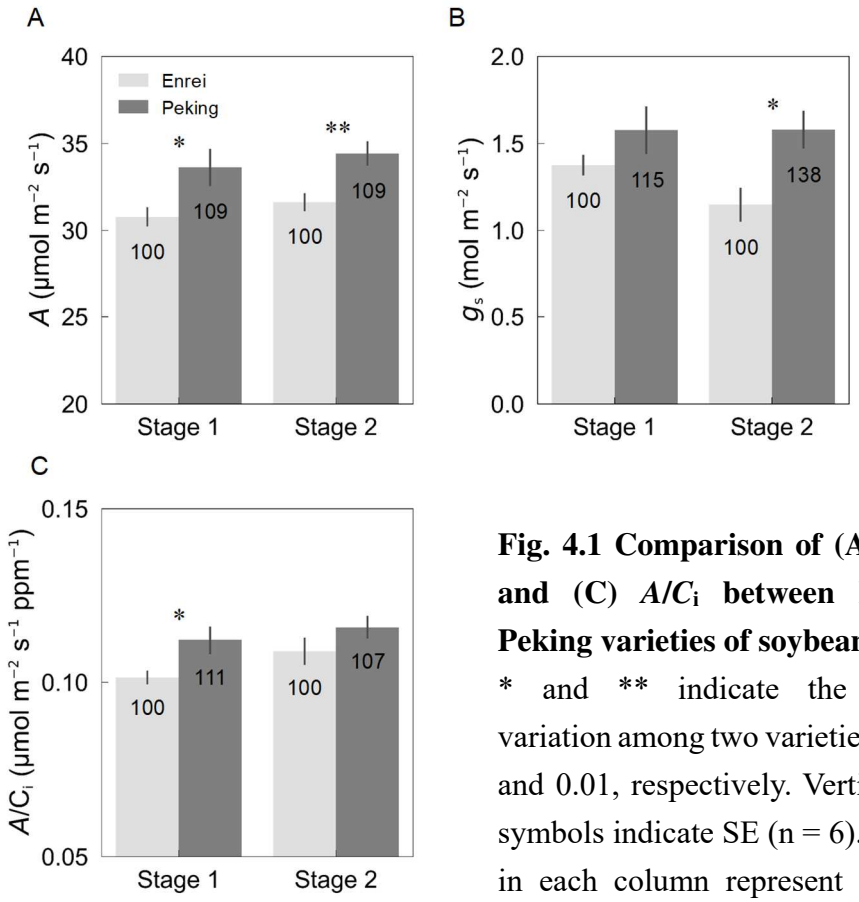

Fig. 4.1 Comparison of (A) *A*, (B) g_s and (C) A/C_i between Enrei and Peking varieties of soybean in 2016.
* and ** indicate the significant variation among two varieties at $p < 0.05$ and 0.01, respectively. Vertical bars on symbols indicate SE (n = 6). The values in each column represent the relative value of Peking to Enrei at each stage.

showed significantly lower *A* than that of Enrei at both growth stages ($p < 0.05$) (Figs. 4.2C and 4.2D). These CSSLs commonly have the P-allele at the SSR marker locus, T002042675s, located on chromosome 20. B0309, which also has the P-allele at T002042675s, showed a lower *A* by 8.7% ($p = 1.00$) and 13.8% ($p = 0.075$) than that of Enrei at Stage 1 and Stage 2, respectively. These results suggest that the QTL related to *A* could exist in the flanking region of T002042675s.

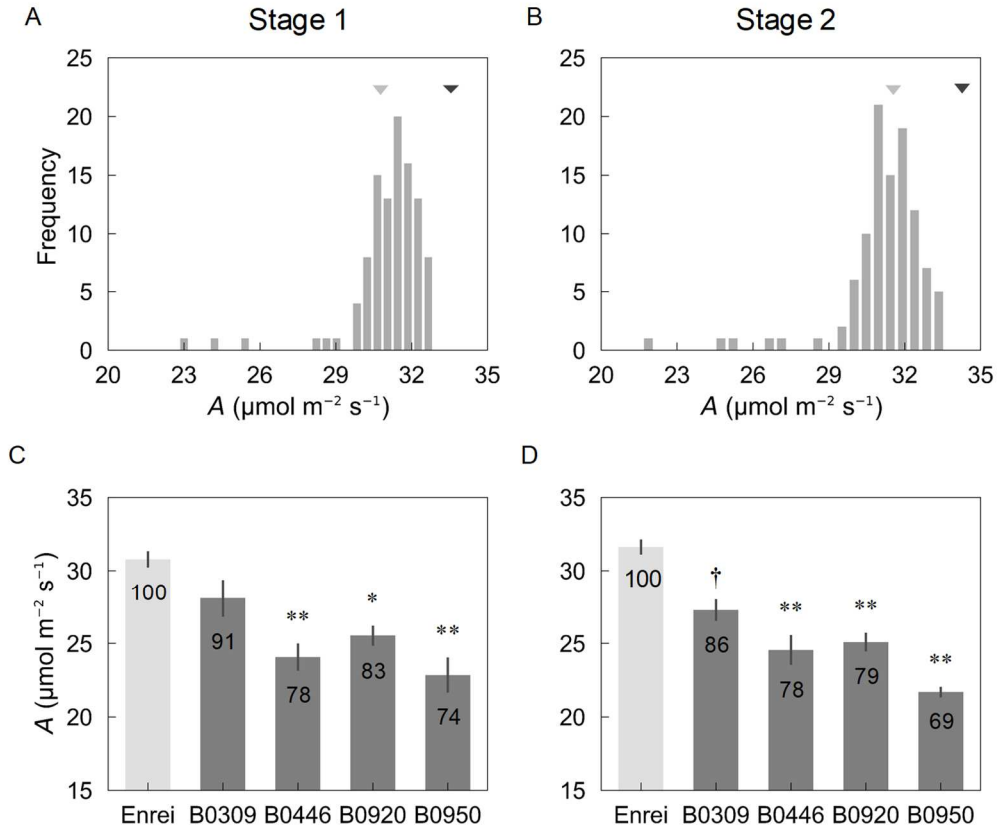

Fig. 4.2 Variation in *A* at (A, C) Stage 1 and (B, D) Stage 2 among the 103 chromosome segment substitution lines (CSSLs).

The gray and black triangles in both figures indicate the value of *A* in Enrei and Peking, respectively. †, * and ** indicate the significant variation between Enrei and each of the four CSSLs at $p < 0.1$, 0.05, and 0.01, respectively, according to the Tukey-Kramer test among Enrei, Peking and 103 CSSLs. Vertical bars on symbols indicate SE (n = 5–6). The values in each column represent the relative value of the CSSL to Enrei at each stage.

In addition, the 21 candidates of QTL with a significant effect on *A* were detected in 2016, according to one-way ANOVA (Table 4.1). The P-allele at eight candidate QTLs

Table 4.1 List of the candidate QTLs for *A* detected by one-way ANOVA.

[a] The position of the QTLs described in Mbp within each chromosome.[b] The effect of the Peking allele on *A* to the Enrei allele at each QTL. ns, not significant at $p < 0.05$; *, significant at $p < 0.05$; **, significant at $p < 0.01$.

Chromosome	QTL name	[a]Position (Mbp)	Flanking marker 1	Flanking marker 2	[b]QTL effect (%)	
					Stage 1	Stage 2
5	*qA_5-1*	2.35 - 3.74	s003503358	s003501972	n. s.	4.5 *
6	*qA_6*	2.12 - 8.78	s002607789	Satt457	n. s.	6.2 *
7	*qA_7*	10.42 - 36.11	Satt323	s019100039	n. s.	3.2 *
11	*qA_11*	8.88 - 10.56	Satt197	GMES0766	3.2 **	n. s.
13	*qA_13-1/qLPC13*	24.45 - 32.87	Satt663	Satt362	3.3 **	6.0 **
16	*qA_16*	35.27 - 37.08	LFsoy6	Sat_395	2.8 *	3.1 *
17	*qA_17-1*	6.16 - 7.81	Satt135	s002507558-2	4.3 *	4.0 *
18	*qA_18-1*	0.11 - 1.34	T001800107s	Satt038	n. s.	3.7 *
3	*qA_3*	38 - 43.53	T0003380041	s006300056	-10.6 ***	-3.4 ***
4	*qA_4*	0.51 - 3.23	Satt565	GMES0757	-7.0 ***	-8.7 ***
5	*qA_5-2*	11.99 - 32.11	T000511990m	s000304457-2	-3.2 *	-3.4 *
8	*qA_8*	38.18 - 43.07	s014700009	GMES0681	-7.1 ***	-8.3 ***
9	*qA_9*	2.86 - 4.16	GMES1693	s008602030	-7.7 ***	-6.8 ***
10	*qA_10*	41.69 - 43.45	s022600099	Satt331	-6.9 *	n. s.
13	*qA_13-2*	40.96 - 44.37	T001340960m	s025500044	-4.9 *	n. s.
14	*qA_14*	44.88 - 47.6	T001444884s	s015600675	-7.1 ***	-5.3 **
17	*qA_17-2*	39.53 - 41.76	s018700334-2	GMES5401	-11.3 ***	-8.7 ***
18	*qA_18-2*	1.74 - 4.64	Satt309-2	T0018046441	-4.8 *	-5.0 *
18	*qA_18-3*	56.7 - 58.72	s002104271	Satt191	-13.9 ***	-14.2 ***
20	*qA_20-1*	0.02 - 0.57	T002000016s	T002000573s	-12.8 ***	-14.2 ***
20	*qA_20-2/qLPC20*	36.01 - 45.55	s013301378-2	Sct_189	-20.0 ***	-21.2 ***

showed positive effects of 2.8–6.2% on *A* throughout both stages, while 13 candidate QTLs showed negative effects of -3.2 to -21.2%. Among eight candidate QTLs with a positive effect, the P-allele at *qA_13-1* showed a significant effect and lowest *p*-value at both stages. The effect of the P-allele at *qA_20-2* was largest of all the candidate QTLs at both growth stages, and *qA_20-2* includes T002042675s detected by the Tukey-Kramer test.

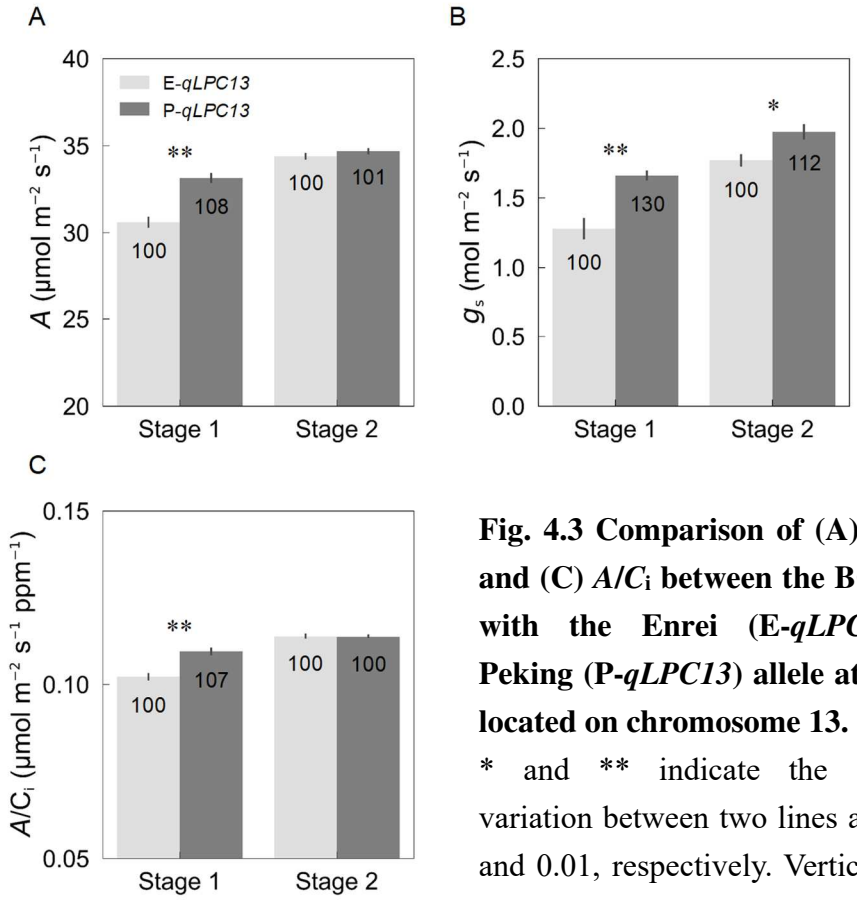

Fig. 4.3 Comparison of (A) *A*, (B) g_s and (C) A/C_i between the BC_3F_4 lines with the Enrei (E-*qLPC13*) and Peking (P-*qLPC13*) allele at the QTL located on chromosome 13.

* and ** indicate the significant variation between two lines at $p < 0.05$ and 0.01, respectively. Vertical bars on symbols indicate SE (n = 9). The values in each column represent the relative value of P-*qLPC13* to E-*qLPC13* at each stage.

These results suggested that *qA_13-1* and *qA_20-2* were the most reliable candidate QTLs with a positive or negative effect, respectively. Thus, I focused on *qA_13-1* and *qA_20-2* and renamed them as *qLPC* (Leaf Photosynthetic Capacity) *13* and *qLPC20*, respectively.

Further, I tested the effect of *qLPC13* and *qLPC20* in 2018, using the four BC_3F_4 lines which were segregated at the flanking region of these candidate QTLs. The BC_3F_4 line with the P-allele at *qLPC13* showed higher A and A/C_i by 8.3% and 7.1%, respectively, than that with the E-allele at Stage 1 (Fig. 4.3) ($p < 0.05$). This line also showed higher g_s by 29.9% and 11.6%, than that with the E-allele at Stage 1 and at Stage 2, respectively ($p < 0.05$). The BC_3F_4 line with the P-allele at *qLPC20* showed a lower A by -8.6% and -15.3%, lower g_s by -30.4% and -45.3%, and lower A/C_i by -6.8% and -12.6% than that with the E-allele at Stage 1 and Stage 2, respectively ($p < 0.05$) (Fig. 4.4). These results confirmed that *qLPC13* and *qLPC20* significantly affected leaf photosynthetic capacity in the Enrei genetic background.

4.3.3 Biochemical and morphological characteristics of the leaf

I analyzed the content of N, Rubisco, and chlorophyll per unit leaf area and *SD* in the soybean lines in 2018. There was no significant variation in the N, Rubisco, and chlorophyll content between Enrei and Peking at Stage 1, although the values of Peking

were significantly lower than those of Enrei at Stage 2 ($p < 0.01$) (Fig. 4.5). Peking showed a higher *SD* by 18.0% than that of Enrei at Stage 1 ($p < 0.01$), while the *SD* was similar at Stage 2. The N content was similar between the BC_3F_4 lines with the E-allele or the P-allele at *qLPC13* at both growth stages (Fig. 4.6).

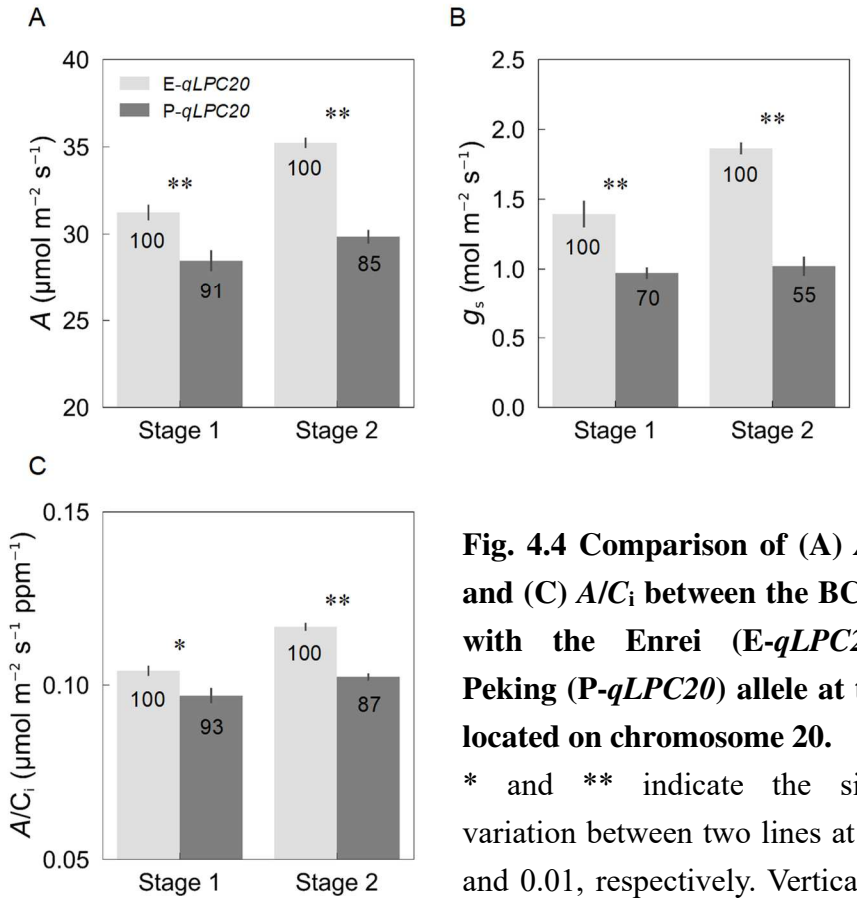

Fig. 4.4 Comparison of (A) *A*, (B) g_s and (C) A/C_i between the BC_3F_4 lines with the Enrei (E-*qLPC20*) and Peking (P-*qLPC20*) allele at the QTL located on chromosome 20.

* and ** indicate the significant variation between two lines at $p < 0.05$ and 0.01, respectively. Vertical bars on symbols indicate SE (n = 9). The values in each column represent the relative value of P-*qLPC20* to E-*qLPC20* at each stage.

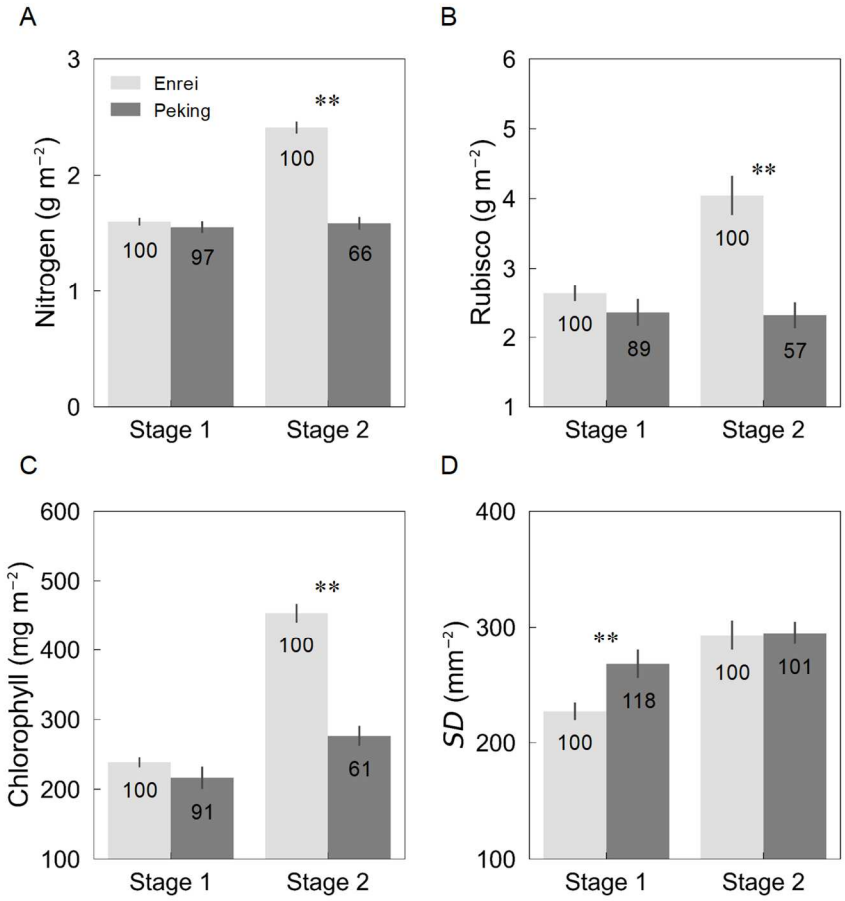

Fig. 4.5 Comparison of the content of (A) N, (B) Rubisco and (C) Chlorophyll, and (D) *SD* between Enrei and Peking varieties of soybean.

** indicates the significant variation between two varieties at $p < 0.01$. Vertical bars on symbols indicate SE (n = 8–9). The values in each column represent the relative value of Peking to Enrei at each stage.

The Rubisco and chlorophyll content of the BC_3F_4 line with the P-allele at *qLPC13* were higher by 16.1% ($p = 0.074$) and 10.8% ($p = 0.155$), respectively, than those with the E-allele at Stage 1. The *SD* of the BC_3F_4 line with the P-allele at *qLPC13* was higher by 11.9% and 10.9% than those with the E-allele at Stage 1 and Stage 2, respectively ($p < 0.05$). There was no significant variation in the N content between the BC_3F_4 lines with

the E-allele or the P-allele at *qLPC20* at Stage 1, while the N content of those with the P-allele was lower by 12.4%than those with the E-allele at Stage 2 (p = 0.056) (Fig. 4.7).

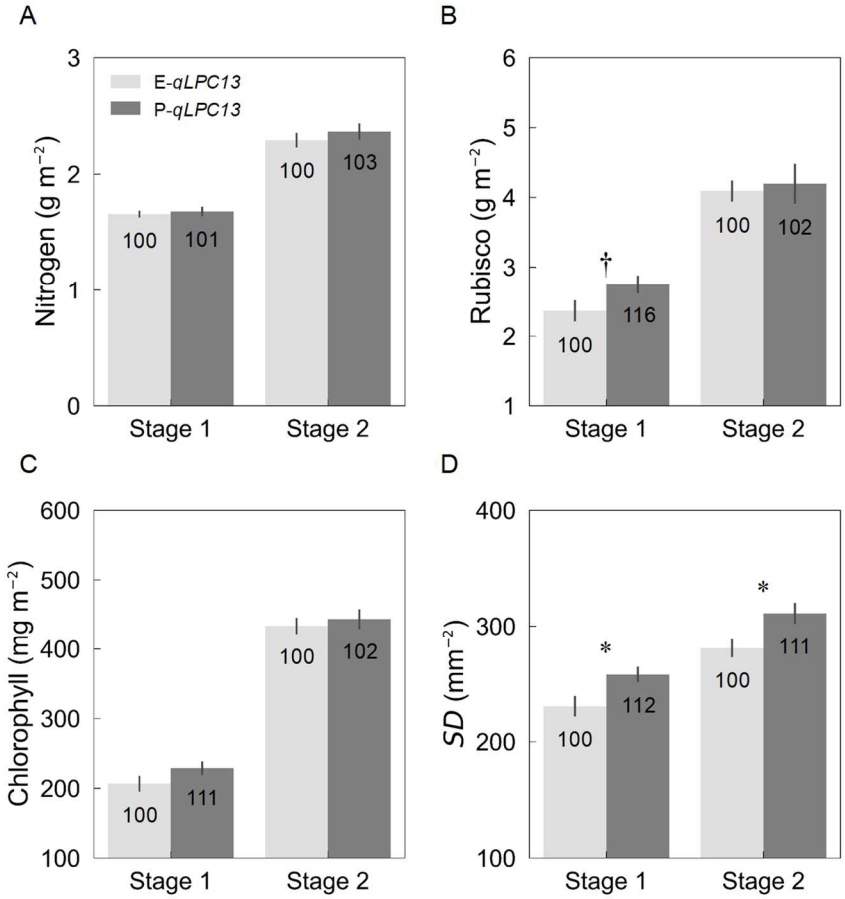

Fig. 4.6 Comparison of the content of (A) N, (B) Rubisco and (C) Chlorophyll, and (D) *SD* between the BC_3F_4 lines with the Enrei and Peking allele at the QTL located on chromosome 13.

† and * indicate the significant variation between two lines at $p < 0.1$ and 0.05, respectively. Vertical bars on symbols indicate SE (n = 9). The values in each column represent the relative value of P-*qLPC13* to E-*qLPC13* at each stage.

The Rubisco and chlorophyll content of the BC_3F_4 line with the P-allele at *qLPC20* were

lower by 12.1% and 15.6%, respectively, than those with the E-allele at Stage 2 ($p < 0.01$), while the variation in these values was not significant at Stage 1. The *SD* of the BC_3F_4 line with the P-allele at *qLPC20* was lower by -10.8% than that with the E-allele at Stage 1 ($p < 0.05$), while the *SD* was similar at Stage 2.

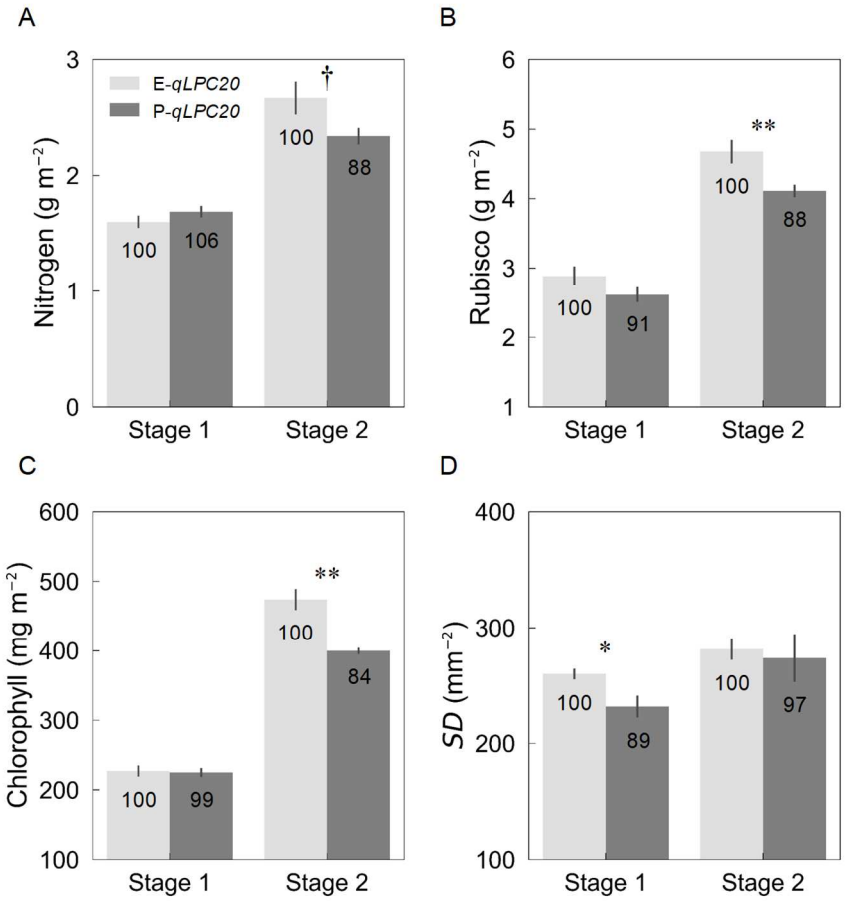

Fig. 4.7 Comparison of the content of (A) N, (B) Rubisco and (C) Chlorophyll, and (D) *SD* between the BC_3F_4 lines with the Enrei and Peking allele at the QTL located on chromosome 20.

†, * and ** indicate the significant variation between two lines at $p < 0.1$, 0.05 and 0.01, respectively. Vertical bars on symbols indicate SE (n = 9). The values in each column represent the relative value of P-*qLPC20* to E-*qLPC20* at each stage.

4.4 Discussion

Previous studies reported significant variation in *A* among various cultivar and landrace soybeans (Ojima, 1972; Butterry et al., 1977; Tanaka et al., 2010; Liu et al., 2012; Koester et al, 2016; Tomeo et al., 2017). They suggested that the observed variation could be attributed to variation in the efficiency of gas diffusion from the atmosphere to the chloroplast or the CO_2 fixation at the chloroplast. In the present study, I revealed greater *A* of Peking than that of Enrei variety of soybean after the flowering stage under field conditions (Figs. 4.1, 4S.1 and 4S.2). The g_s and A/C_i of Peking tended to be higher than those of Enrei, which may contribute to the higher *A*. The potential of the g_s can be mainly determined by the morphological characteristics of the stomata (Franks and Breeling., 2009). In soybean, *SD* was reported to strongly correlate with the potential of g_s among 77 cultivars (Tanaka et al., 2010). Moreover, g_s can be largely affected by the water status in the plant (Flexas et al., 2004). In the present study, the g_s and *SD* were significantly higher in Peking than Enrei at Stage 1 in 2018 (Figs. 4.5 and 4S.2). The g_s was evaluated in all the soybean lines under favorable water conditions by irrigation. These results suggest that the higher g_s can be partly attributed to the higher *SD* in Peking.

The A/C_i can reflect the efficiency of gas diffusion inside the leaf and CO_2 fixation at the chloroplast. At the current atmospheric [CO_2], CO_2 fixation can be limited by the

carboxylation of ribulose-1,5-bisphosphate catalyzed by Rubisco in plants (Farquhar et al., 1980). In the present study, A/C_i of Peking was significantly higher than that of Enrei, even though the N, Rubisco, and chlorophyll content of Peking was similar or slightly lower than that of Enrei at Stage 1 in 2018 (Figs. 4.5 and 4S.2). These results indicate that Peking might have higher efficiency in gas diffusion from the intercellular space to the chloroplast (g_m), or a higher activation state of Rubisco than that of Enrei. In Chapter 3, Peking showed greater g_m than Enrei under the field condition. The increase in the g_m can improve the water use efficiency for photosynthesis unless the g_s and g_m change in parallel (Flexas et al., 2013; Tomeo et al., 2017). The higher activation state of Rubisco can maintain leaf photosynthetic capacity with less N investment to Rubisco, which might improve the N use efficiency for photosynthesis. In fact, the CO_2 assimilation rate per unit of N in the Peking variety was higher by 15.2% and 54.0% than those of Enrei at Stage 1 and Stage 2, respectively (Fig. 4S.4) ($p < 0.01$). Therefore, Peking can be the useful material to breed a soybean cultivar with high efficiency of water and N use.

In soybean, the QTLs related to *A* have been identified on chromosome 10 and 16 by Vieira et al., (2006), on chromosome 4, 10, 15 and 17 by Yin et al., (2010), and on chromosome 9 and 12 by Li et al., (2016). In the present study, I identified two QTLs with a significant effect on *A* located on chromosome 13 (*qLPC13*) and 20 (*qLPC20*). To

the best of our knowledge, this is the first report that identifies the genetic factors affecting leaf photosynthesis in field-grown soybeans. *qLPC13* and *qLPC20* exist within 26.5 to 32.9 Mbp on chromosome 13 and within 39.9 to 42.7 Mbp on chromosome 20, respectively. They are not consistent with the QTLs reported by previous studies on leaf photosynthesis; however, the effect of the QTL is known to be influenced by the environmental conditions and genetic background being examined (Wang et al., 2014). The present study differed from these previous studies in terms of the environmental conditions and the genetic background of the soybean populations for the QTL analysis, which might be responsible for the inconsistency in the detected QTLs.

Nine and two major genes controlling the maturity (Li et al., 2016; Lu et al., 2017) and the stem growth habit (Bernard, 1972), respectively, have been reported in soybean. These genes are shown to affect not only the phenology and the stem growth habit but also many physiological aspects of the plant (Watanabe et al., 2012). Tanaka et al., (2009) reported that the stem growth habit significantly affected the potential of g_s in soybean through the effect on leaf morphology related to the stomata. In the present study, the importance of *qLPC13* and *qLPC20* are not consistent with any previously identified genes. The R1 and R5 date was similar between the BC_3F_4 lines with the E-allele or the P-allele at *qLPC13*, or those at *qLPC20*, respectively, in 2018 (Table 4S.3). In addition, the stem growth habit

was the same in these four lines. These results indicate that the effect of *qLPC13* and *qLPC20* are not pleiotropic effects of the genes influencing the phenology or the stem growth habit in soybean.

The P-allele at *qLPC13* significantly increased *A* in the Enrei genetic background, indicating that *qLPC13* can contribute to a high capacity for leaf photosynthesis in Peking. On the other hand, the P-allele at *qLPC20* significantly decreased *A*. It is possible that the negative effect of the P-allele at *qLPC20* can be specifically expressed in the Enrei background but not in the Peking background, or that such negative effect can be offset by the other genetic factors with a positive effect on *A* in the Peking background. Compared with *qLPC13*, the effect of the P-allele at *qLPC20* was stable and large after the flowering stage in 2016 and 2018 (Figs. 4.2, 4.3 and 4.4). *qLPC20* was close to or overlapped with the QTL, which showed the significant effect on the seed weight per plant and/or 100-seeds weight in the genetic background of Enrei and Peking (Watanabe et al., 2018), and other backgrounds (Yuan et al., 2002; Kabelka et al., 2004; Han et al., 2012). These results suggest that *qLPC20* has the significant effect on leaf photosynthetic capacity, which may even impact the seed yield in soybean.

To elucidate the physiological aspects of the QTL effect on leaf photosynthesis, I analyzed the biochemical and morphological traits related to leaf photosynthesis in the

BC_3F_4 lines with similar genetic background except for *qLPC13* or *qLPC20*. The effect of the P-allele at *qLPC13* on g_s was 29.9% and 11.6% at Stage 1 and Stage 2 in 2018, respectively ($p < 0.05$) (Fig. 4.3B), while the effect on *SD* was 11.9% and 10.9% at Stage 1 and Stage 2 in 2018, respectively ($p < 0.05$) (Fig. 4.6D). Thus, the P-allele at *qLPC13* can have the positive effect on *SD*, which might result in greater g_s. The effect of the P-allele at *qLPC13* on the A/C_i was 7.1% at Stage 1 in 2018 ($p < 0.01$) (Fig. 4.3C). The Rubisco and chlorophyll content per unit leaf area tended to be higher in the BC_3F_4 line with the P-allele at *qLPC13* than for those with the E-allele, while the N content was quite similar (Fig. 4.6). These results suggest that the P-allele at *qLPC13* can increase the A/C_i due to more N distribution to the photosynthetic apparatus, which can contribute to greater *A*, at least during the specific growth stage. This could result in the higher CO_2 assimilation rate per unit of N in the BC_3F_4 line with the P-allele at *qLPC13* than for those with the E-allele at this stage (Fig. 4S.4B). Therefore, the P-allele at *qLPC13* can be exploited by soybean breeding to improve leaf photosynthetic capacity as well as the N use efficiency.

The P-allele at *qLPC20* significantly decreased the Rubisco and chlorophyll content only at Stage 2 in 2018 (Fig. 4.7). This is partly consistent with the larger decrease in the A/C_i at Stage 2 than at Stage 1 in the BC_3F_4 line with the P-allele at *qLPC20*. The N

content of the BC_3F_4 line with the P-allele at *qLPC20* was 12.4% lower than that with the E-allele at Stage 2 (p = 0.056). It indicates that the P-allele at *qLPC20* can decrease the N accumulation in the leaf, which might result in the reduction in the Rubisco and chlorophyll content at Stage 2. The P-allele at *qLPC20* significantly decreased the *SD* only at Stage 1, although the decrease in the g_s was much larger at Stage 2 than that at Stage 1 in the BC_3F_4 line with the P-allele at *qLPC20*. It was reported that an N deficiency can reduce the stomatal aperture due to the increase in the sensitivity to abscisic acid and the declining water status in plants (Radin et al., 1982; Ishikawa-Sakurai et al., 2014). Thus, the decrease in the N content could be one of the causes for the considerable reduction in the g_s observed in plants with the P-allele at *qLPC20* at Stage 2. Further study is needed to reveal the physiological mechanism of the effect of *qLPC13* and *qLPC20* on leaf photosynthesis in detail.

In summary, I confirmed a greater rate of CO_2 assimilation (A) in Peking than that in Enrei varieties of soybean after the flowering stage under field conditions in Chapter 4. The genetic analysis identified two novel QTLs, *qLPC13* and *qLPC20*, related to the variation in A between Enrei and Peking. This is the first report to identify the genetic factors affecting leaf photosynthetic capacity in field-grown soybean. The Peking allele (P-allele) at *qLPC13* had a positive effect on the efficiency of both the gas diffusion via

the stomata and the CO_2 fixation at the chloroplast, which resulted in greater *A* in the genetic background of Enrei. On the other hand, the P-allele at *qLPC20* had a negative effect on these physiological traits, which resulted in the significant reduction in *A*. These QTLs identified in the present study provide a significant advance in the understanding of the genetic mechanism underlying leaf photosynthesis in field-grown soybeans. The identification of the causal genes in these QTLs can provide a novel strategy to enhance leaf photosynthetic capacity with soybean breeding.

Table 4S.1. List of the SSR markers used for the genotyping.

Chromosome	SSR marker	Position (Mbp)	Primer sequence	
			Forward	Reverse
13	Sat_234	26.5	ATGCGTTTAATAAGTTTTGAAAAATGCC	GAAACCATCCTTATATGTCAATTGCTCA
	Satt114	27.7	GGGTTATCCTCCCCAATA	ATATGGGATGATAAGGTGAAA
	s017200718	29.1	CAAGACAATAATGCTGTAAACATAAA	CGTCGACACGTGTATCATTGTAT
	Satt335	31.5	CAAGCTCAAGCCTCACACAT	TGACCAGAGTCCAAAGTTCATC
	Satt362	32.9	TTGTTGTTTCAAATGTATTTTAGTT	GACGGATCATCAAACCAATCAAGAC
20	Sat_324	39.9	CAATGTCCCTCTTTCTTCCAATGATAA	TGCAGGGGAGATTAGCTAGAAATGTG
	T002042675s	42.7	TAATTGTGGACTTCAAAGAAGGG	TTGATTGGGAATTCGTTTCTACA

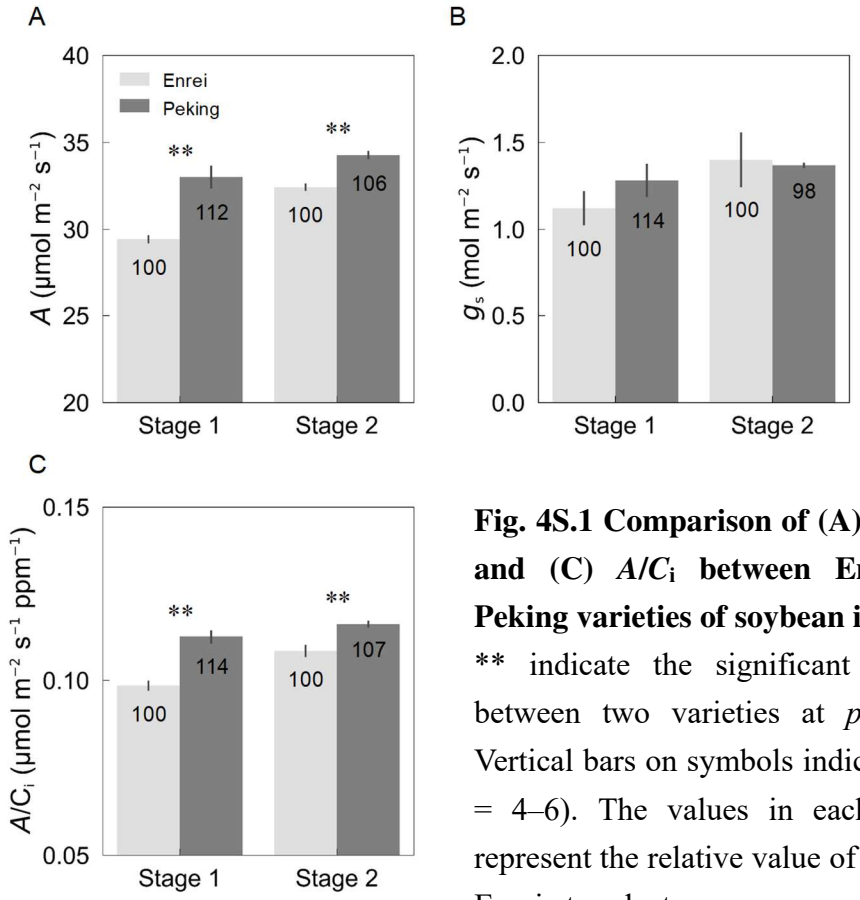

Fig. 4S.1 Comparison of (A) *A*, (B) g_s and (C) A/C_i between Enrei and Peking varieties of soybean in 2017.
** indicate the significant variation between two varieties at $p < 0.01$. Vertical bars on symbols indicate SE (n = 4–6). The values in each column represent the relative value of Peking to Enrei at each stage.

Table 4S.2 Phenology of Enrei and Peking soybean varieties.

Year	Enrei		Peking	
	R1	R5	R1	R5
2016	35	48	33	54
2017	34	51	35	55
2018	34	51	39	58

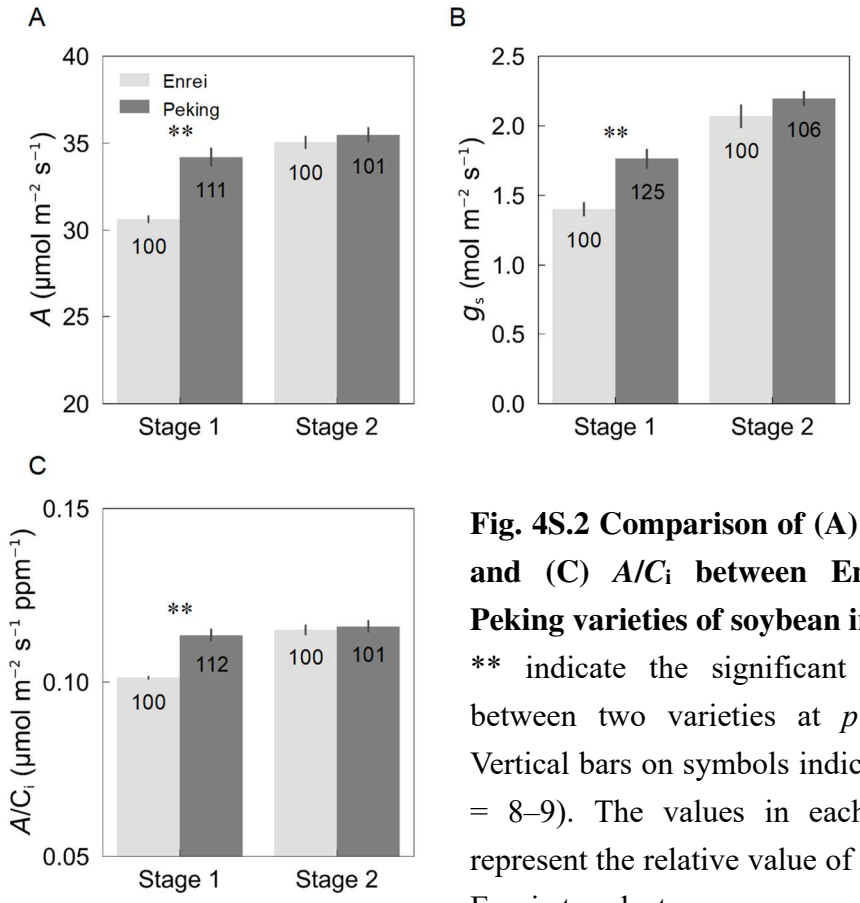

Fig. 4S.2 Comparison of (A) *A*, (B) g_s and (C) A/C_i between Enrei and Peking varieties of soybean in 2018. ** indicate the significant variation between two varieties at $p < 0.01$. Vertical bars on symbols indicate SE (n = 8–9). The values in each column represent the relative value of Peking to Enrei at each stage.

Table 4S.3 Phenology of the BC_3F_4 lines with the Enrei or Peking allele at the QTL located on the chromosome 13 and 20.

QTL name	*qLPC13*		*qLPC20*	
allele	Enrei	Peking	Enrei	Peking
R1	32	33	33	32
R5	50	51	49	48

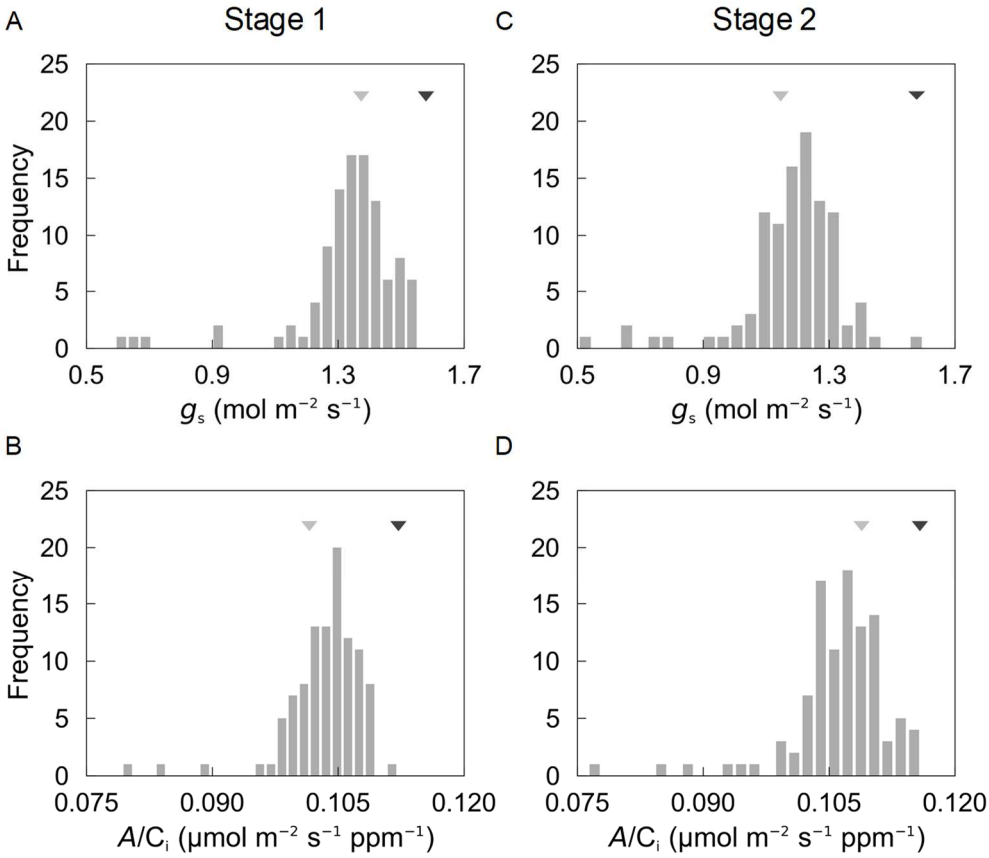

Fig. 4S.3 Variations in g_s and A/C_i at (A, B) Stage 1 and (C, D) Stage 2 among the 103 CSSLs.

The gray and black triangles in both figures indicate the value of g_s and A/C_i in Enrei and Peking, respectively.

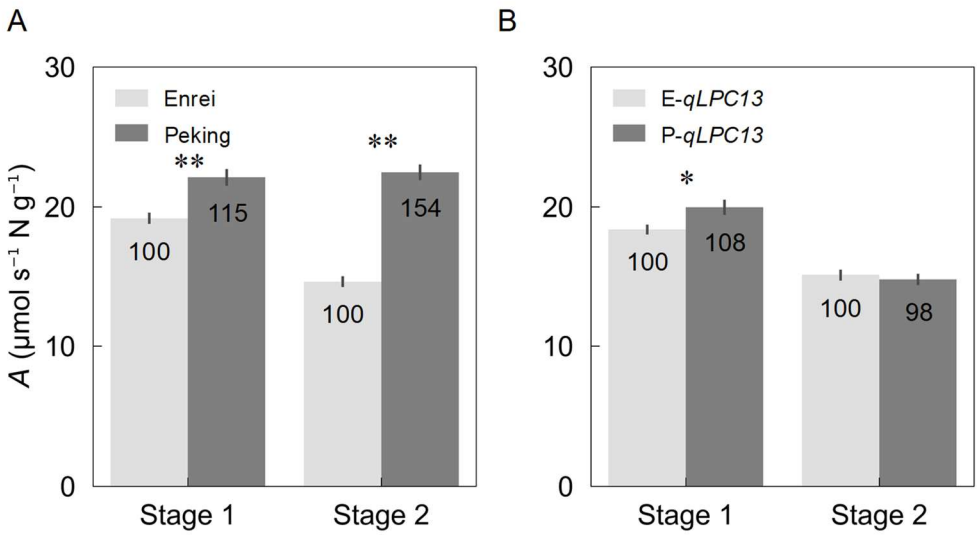

Fig. 4S.4 Comparison of the CO_2 assimilation rate per unit of nitrogen in (A) Enrei and Peking, and (B) E-*qLPC13* and P-*qLPC13*.

* and ** indicate the significant variation between two varieties at $p < 0.05$ and 0.01, respectively. Vertical bars on symbols indicate SE (n = 8–9). The values in each column represent the relative value of (A) Peking to Enrei or (B) P-*qLPC13* to E-*qLPC13*, respectively, at each stage.

Chapter 5

General discussion

5.1 Potential targets to enhance leaf photosynthesis in plant species

Enhancing leaf photosynthesis can be a novel pathway to drive further increase in crop yield (von Cammerer and Evans, 2010). This section introduces the physiological traits related to leaf photosynthesis, which has been identified as a promising target for this attempt. As for the enhancement of the CO_2 fixation, the enzymes involved in Calvin cycle can be feasible targets. Rubisco is considered as the key enzyme to enhance leaf photosynthesis in C_3 plants, since it can limit leaf photosynthesis at the current atmospheric CO_2 concentration (Farquhar et al., 1980). The limitation of photosynthesis by Rubisco results from the low catalytic turnover rate (k_{cat}) and competing oxygenation reaction of Rubisco in C_3 plants. On this background, the modification of the kinetic properties has been attempted in plant species (Suzuki et al, 2007; Whitney and Andrew, 2011). Altering the protein distribution among the photosynthetic proteins in Calvin cycle can be also a promising strategy (Raines, 2011). A modeling analysis suggested that the increase in the amount of sedoheptulose-1,7-bisphosphatase (SBPase) and ADP glucose

pyrophosphorylase and the decrease in that of photorespiratory enzymes can achieve greater *A* in C_3 plants (Zhu et al., 2007). Lefebvre et al., (2005) reported that the transgenic line with the increased SBPase activity showed higher *A* and biomass yield than wild-type line in tobacco. In soybean, the soybean line expressing the cyanobacterial Fructose 1,6-bisphospatase (FBPase)/SBPase showed greater *A* and stability of the seed yield to the environmental changes predicted in the future than the wild-type line of soybean, indicating the manipulation of the photosynthetic carbon reduction cycle by the genetic engineering can be effective to improve the soybean production (Köhler et al., 2017). Moreover, concentrating [CO_2] in the chloroplast can be the other pathway to enhance leaf photosynthesis by introducing the C_4 pathway and Kranz anatomy in C_3 plants or the [CO_2] concentrating system of cyanobacteria (Hibberd et al., 2008; Lieman-Hurwitz et al., 2003). It can, theoretically, result in the inhibition of photorespiration, which can reduce the energy loss in photosynthesis among C_3 plants.

The gas diffusion resistance from the atmosphere to the chloroplast can be the limiting factors for leaf photosynthesis in plants (Sharkey, 1982). The gas diffusion conductance via the stomata (g_s) has been shown to correlate with *A* among crop species (Fischer et al., 1998; Kanemura et al., 2007; Ohsumi et al., 2007; Tanaka et al., 2010). The potential of g_s can be determined by the size, depth, opening of a single stoma, and its density

(Franks and Breeling, 2009). Previous studies have provided the advanced insight into the genetic mechanisms underlying stomatal development and movement, which provides the opportunity to manipulate the stomatal characteristics. Stomatal opening is regulated by at least three key components, blue right receptor phototropin, plasma membrane H^+-ATPase and plasma membrane inward rectifying K^+ channels in the guard cell (Inoue and Kinoshita, 2017). The activation of H^+-ATPase induced by blue light as the initial signal facilitates the K^+ uptake through the inward rectifying K^+ channel to increase the turgor pressure of guard cells, which results in stomatal opening. It was shown that the overexpression of *AHA2*, coding Araibdopsis *H^+-ATPase* in the guard cell, and that of *PATROL1*, controlling the translocation of a major H^+-ATPase to plasma membrane, increased g_s, A and biomass yield in Arabidopsis (Wang et al., 2014; Hashimoto-Sugimoto et al., 2013). Stomatal development is tightly regulated by various signals influenced by plant hormones and environmental stimuli in plants. An *SDD1* knockout line of Arabidopsis with the increased stomatal density (*SD*) was reported to show greater g_s than wild-type line, depending on the light condition (Schlüter et al., 2003). In addition, Tanaka et al., (2013b) suggested that the increased *SD* by overexpressing *STOMAGEN*, the positive intercellular signaling factor for stomatal differentiation, contributed to the increase in g_s and A under the saturated-light condition in Arabidopsis. In soybean, it was

shown that the variation in *SD* would be a major determinant of that in the potential for the g_s among 77 soybean varieties (Tanaka et al., 2010). These facts suggest that the manipulation of the stomatal opening and development can be the promising pathway to enhance leaf photosynthetic capacity in crop plants.

The gas diffusion conductance from the intercellular spaces to the chloroplast (g_m) can attribute the significant limitation to *A* with the similar extent to g_s (Pons et al., 2009). The gas diffusion pathway inside the leaf is composed of the gaseous and liquid phases, and the resistance in the liquid phase can be relatively large in general. It was shown that g_m was correlated with the surface area of chloroplasts exposed to intercellular spaces, indicating that chloroplast allocation in the mesophyll cell can largely affect CO_2 diffusion efficiency inside the leaf (Evans, 1999). The thickness of the mesophyll cell wall is known to have the large resistance for CO_2 diffusion, accounting for up to 50% of total resistance (Evans et al., 2009). In addition, the CO_2 permeability via plasma membrane and chloroplast envelope can be a major component of the resistance. It was reported that two aquaporins, AQP1 and PIP1 which have the function as a water channel, facilitated the CO_2 transportation via the membranes (Flexas et al., 2006). Hanba et al., (2004) identified the increase in g_m as well as *A* and g_s due to the overexpression of the barley aquaporin, HvPIP2;1, in rice. Interconversion between CO_2 and bicarbonate

catalyzed by carbonic anhydrase (CA) can facilitate the CO_2 transport across the chloroplast. Overall, g_m can be determined by these morphological and biochemical characteristics of the leaf, which can be the target to enhance leaf photosynthetic capacity. The large variation in *A* within or among crop species can be exploited to improve *A* by elucidating the mechanisms underlying such variation (Flood et al., 2011). That variation is attributable to the variation in the physiological traits mentioned above. These physiological traits have been attempted to be modified by manipulating the expression level of the relevant genes or introducing those genes from different or same species. The genetic engineering has been utilized to introduce the foreign genes to a plant species, which can realize the drastic change in the plant phenotype. However, the implementation of the genetic engineering for the crop breeding program faces the significant barrier from the point of view of technical, ethical and social problems, and, thus, seems to be a long-time goal.

5.2 Promising strategies to enhance leaf photosynthesis of soybean by utilizing the natural variation

In the crop breeding, marker-assisted selection (MAS) has been an efficient and practical method for the introgression of the useful alleles associated with important agronomical

traits (Wang et al., 2012). The genetic analysis, such as QTL analysis and genome-wide associate study, enables us to identify the causal genes and alleles for the variation in traits of interest among a single or relative crop species, which provides the target with the breeding program based on MAS. Previous studies elucidated the genetic factors related to the variation in *A* among the varieties of several crop species (Flood et al., 2011). In rice, two causal genes for such variation were identified (Takai et al., 2013; Adachi et al., 2017), which achieves the enhancement of leaf photosynthetic capacity by the introgression of the superior allele by MAS (Adachi et al., 2013). Thus, the combining method of the genetic analysis and MAS can be the effective strategy to enhance leaf photosynthetic capacity directly towards the yield improvement in crop species. In the present study, I identified two novel QTLs, *qLPC13* and *qLPC20*, related to the variation in *A* between Enrei and Peking (Chapter 4). This is the first report of QTLs affecting leaf photosynthesis in field-grown soybeans, and will enable the genetic improvement of leaf photosynthesis through the breeding program based on MAS in soybean.

Previous studies reported the several QTLs related to the seed yield in soybean, although the causal genes in these QTLs are still unrevealed (Orf et al., 1999; Yuan et al., 2002; Kabelka et al., 2004; Guzman et al., 2007; Han et al., 2012). Concibido et al., (2003) identified the QTL from *Glycine soja* enhancing the seed yield by 9% in the genetic

background of soybean. However, the effect of this QTL was confirmed in only the limited soybean varieties, which requires the characterization of the causal gene and the physiological mechanism underlying the gene function. The QTL, *qLPC20* identified in the present study, is close to or overlapped with one of the yield-related QTLs detected in several soybean populations with different genetic backgrounds (Yuan et al., 2002, Kabelka et al., 2004, Han et al., 2012, Watanabe et al., 2018). It suggests that the causal gene in *qLPC20* can have a significant effect on leaf photosynthetic capacity and the seed yield among soybean varieties with various genetic backgrounds. I already have narrowed down the candidates to less than 30 genes existed in *qLPC20* (data not shown). The identification of the causal gene can provide an advanced insight into the genetic and physiological basis underlying the determination of the soybean yield.

5.3 Ideal characteristics related to leaf photosynthesis of soybean under the future environment

The global CO_2 concentration in the atmosphere has been continuously risen from 280 ppm in 1750 before the industrial era to 405 ppm in 2018, and it is projected to reach up to 550–950 ppm by 2100 (IPCC, 2018). Under such elevated [CO_2] condition, leaf photosynthesis can be limited by the regeneration of RuBP or the availability of

triphosphate in the chloroplast (Farquhar et al., 1980; Sharkey et al., 1985). It indicates that the typical amount of Rubisco adapting the current [CO_2] condition can be excessive in the plant leaves under the future environmental condition. It was suggested that 65% of the Rubisco content comparing with wild-type line could be optimum in rice to realize the greater N use efficiency for leaf photosynthesis under the CO_2 concentration of 100–115 Pa (Makino et al., 1997). Kanno et al., (2017) showed that the even 10–20% decrease in the Rubisco content resulted in the improvement of *A* and the biomass yield under such elevated [CO_2] condition. These results evidence that the optimization (i.e. the reduction) of the Rubisco content can be a possible strategy to enhance the crop production in the future.

In the present study, I showed that the N and Rubisco content per unit leaf area increased drastically, while *A* and A/C_i were relatively constant throughout the reproductive stage in soybean (Chapter 3). This inconsistency could be attributed to a decrease in the activation state of Rubisco with the increase in the N and Rubisco content during this stage. The activation state of Rubisco ranged 80–100% in other crop plants under high-light and ambient [CO_2] condition, whereas it decreased to 50–60% during the reproductive stage among soybean varieties in the present study (Fukayama et al. 2012; Carmo-Silva et al. 2012). It implies that the Rubisco amount in soybean leaf can

be excessive as compared to that of other components related to the RuBP regeneration during the later growth stage even under the current CO_2 concentration. Thus, the optimization of the Rubisco content can improve leaf photosynthetic capacity as well as the N use efficiency due to the superior N allocation among the photosynthetic proteins in soybean leaves under the current and future [CO_2] conditions. At present, I am developing the soybean mutant lines with the decreased Rubisco content in the leaf (data not shown). Further study using these mutant lines will explore the potential to enhance the biomass productivity and N use efficiency by optimizing the Rubisco content in soybean, which will contribute to the sustainable production of soybean in the future.

The soybean production can be threatened by severe stresses from high temperature and drought under the future environment, which requires the enhancement of the water use efficiency (WUE) in soybean breeding. The enhancement of g_m can improve WUE unless g_s and g_m changes in parallel (Flexas et al., 2013). It was, on the other hand, reported that the variation in g_s and g_m among soybean varieties was positively correlated, unlike among wheat varieties (Barbour et al., 2016; Tomeo et al., 2017). In addition, both of g_s and g_m tended to be higher in the soybean varieties with greater A among soybean varieties in the present study. These results suggest that the determination of g_s and g_m can be highly correlated in soybean. The elucidation of the mechanism underlying the

relationship between the g_s and g_m determination is crucial to improve WUE by the g_m enhancement in soybean. Another pathway to improve WUE include the reduction in *SD* in soybean (Tanaka et al., 2010). It was shown that the decrease in *SD* improved the tolerance to drought and high temperature stresses since the exceeded water loss via the stomata could be suppressed in rice (Caine et al., 2018). It suggests that the reduction in *SD* can be an adapted anatomical character of the leaf to the future environmental condition, whereas it should take into the consideration that any reduction of stomatal conductance causes the declines in the CO_2 assimilation and transpiration which has the function to transport of solutes in different parts of the plant body and to maintain appropriate leaf temperature by the cooling effect (Caird et al., 2007).

5.4 Temporal characteristics of leaf photosynthesis in nature

There are not a few studies that showed no clear or even negative correlation between leaf photosynthetic capacity and the seed yield among several crop species, although such relationship was observed among the varieties differing in many physiological aspects beyond leaf photosynthesis (Evans, 1993). This inconsistency can reflect the complexity of the yield determination in crops under the field condition. A large portion of the studies for photosynthesis have focused on the photosynthetic capacity under the steady-state

condition on a specific leaf position at the limited growth stages in the crop development (Long, 1998). However, environmental conditions, such as light intensity, temperature and humidity, are constantly and drastically changing and crop plants are growing with adapting such changing conditions during their growth period. Therefore, the understanding of spatial and temporal characteristics of photosynthesis through the crop development should be important to suggest a novel strategy for the yield improvement in crop species.

Under the field condition, light intensity can be fluctuated with the scales from a few seconds to minutes over the course of a day due to the changing in the solar radiation, cloud cover or self-shading in the crop canopy. Leaf photosynthetic rate gradually increases after the transition from low to high light intensity, and this phenomenon is called as 'photosynthetic induction response'. The rapidity of photosynthetic induction response can be mainly limited by both the Rubisco activation and the stomatal opening among several plant species (Soleh et al., 2016). It was suggested that Rubisco activase, which regulates the ATP-dependent Rubisco activation, can be the promising target for the improvement of photosynthetic induction response (Yamori et al., 2012; Carmo-Silva and Salvucci, 2013). In addition, the overexpression of *PATROL1* resulted in the faster response of g_s to the changing light intensity in Arabidopsis, which can also achieve the

faster response of A (Hashimoto-Sugimoto et al., 2013). Further study is expected to investigate the induction response of g_m since it has never elucidated, although g_m attributes the significant limitation to A in plants. A simulation analysis demonstrated that the loss of the potential cumulative amount of CO_2 assimilation can reach at least 21% due to the slow response of photosynthetic induction to the fluctuating light (Taylor and Long, 2017). The enhancement of photosynthetic induction response can achieve the more efficient carbon gain under the field condition, which will open a new pathway to improve the biomass production in crop species.

Previous studies investigated the diurnal change of A in soybean and reported the declining of A in midday even under the high-light intensity (Kokubun and Shimada, 1994a; Koester et al., 2016). The diurnal change in A and g_s is often correlated, indicating that the stomatal behavior can be a major determinant of the diurnal change in A among several plant species (Matthews et al., 2017). The stomatal behavior can be mainly regulated by the water status in the leaf, the aqueous signals from mesophyll cells and the sucrose metabolism to maintain the balance between the CO_2 assimilation and water use in plants (Fujita et al., 2013). Kokubun and Shimada (1994a; 1994b) reported that Peking showed the lower seed yield than the other commercial varieties. Peking is a landrace from China and might have not experienced the severe selection for the seed yield

throughout the breeding process, which might be one of the reasons for the low yield of Peking. On the other hand, these studies reported that Peking showed higher g_s and A by maintaining the higher water potential of the leaf over a day than the other soybean varieties including Enrei, which might contribute to the greater stability of the seed yield under the field condition. In the present study, Peking showed greater g_s and A than the other varieties after the reproductive stage. These results suggest that Peking can maintain the high level of leaf water potential independently of environmental conditions, which can be beneficial to stabilize the biomass productivity, especially under drought stress. The QTL, *qLPC13* identified in the present study, can relate to this advantage in Peking since the Peking allele at *qLPC13* significantly increased g_s after the flowering stage (Fig. 4.4).

5.5 Conclusion

The present study identified three soybean varieties with the high capacity for leaf photosynthesis among soybeans. The high photosynthetic capacity of these varieties can be attributed to high g_s, g_m, or Vc_{max}, demonstrating that the several physiological traits can be the promising targets to enhance leaf photosynthetic capacity in soybean. In addition, the genetic analysis using the CSSLs revealed two novel QTLs related to leaf

photosynthetic capacity of soybean. The understandings obtained in the present study give us the advanced insight into the physiological and genetic mechanisms underlying leaf photosynthetic capacity of soybean and will open a novel pathway enhancing the photosynthetic capacity towards the yield improvement in soybean breeding.

Acknowledgement

My doctoral thesis was completed after the study for five years at the Laboratory of Crop Science, Graduate School of Agriculture, Kyoto University. I would like to offer my special thanks to the following people for assisting my research. Firstly, my deepest appreciation goes to Prof. Tatsuhiko Shiraiwa and Dr. Yu Tanaka for their supervision of my doctoral thesis, and valuable and insightful suggestions. I received generous supports from them. I am also deeply grateful to Dr. Tomoyuki Katsube-Tanaka (Kyoto University) and Prof. Koki Homma (Tohoku University) for their constructive suggestions during the course of my study.

I would like to express my gratitude to Dr. Hiroshi Fukayama (Kobe University), Kaga Akito (NARO) and Masao Ishimoto (NARO) for their corporation and gracious supports in my thesis. My appreciation should be taken to Prof. Stephen P. Long (University of Illinois), Prof. Randall Nelson (USDA-ARS) and Dr. Johannes Kromdijk (University of Cambridge) for their support on the study at University of Illinois, Urbana-Champaign and Prof. Jeffery D. Ray (USDA-ARS) for providing plant materials. I have greatly benefited from Dr. Sho Ohno (Kyoto University) for assistance in analyzing leaf anatomical structure and Dr. Yoshitaka Takano (Kyoto University) for assistance with the protein analysis in Chapter 3. A part of this study was supported by the project of Research fellow of the Japan Society for the Promotion of Science for Young Scientists.

I never forget my special thanks to Dr. Kenichiro Fujii (NARO), Dr Yohei Kawasaki (NARO), Dr. Yoshihiro Hirooka (Kinki University) and Dr. Kazuhiko Fujisao (NARO), Mr. Seita Suzuki (Kyoto University) and all the members of the Laboratory of Crop Science at Kyoto University for the collaborative work and their insightful suggestions for my study. I owe my great gratitude to Mr. Ryoichi Wada and Mr. Norishige Okamoto for the committed support on the management of the field experiments.

Finally, my deep appreciation goes to my parents, sister, brothers, relatives and all the friends for their support. I could never complete my thesis without their encouragements and assistances.

Kazuma Sakoda

References

Adachi S., Tsuru Y., Nito N. et al., 2011a. Identification and characterization of genomic regions on chromosomes 4 and 8 that control the rate of photosynthesis in rice leaves. Journal of Experimental Botany **62**, 1927–1938.

Adachi S., Nito N, Kondo M. et al., 2011b. Identification of chromosomal regions controlling the leaf photosynthetic rate in rice by using a progeny from japonica and high-yielding indica varieties. Plant Production Science **14**, 118–127.

Adachi S., Nakae T., Uchida M., et al. 2013. The mesophyll anatomy enhancing CO_2 diffusion is a key trait for improving rice photosynthesis. Journal of Experimental Botany **64**, 1061–1072.

Adachi S., Yoshikawa K., Yamanouchi U., et al., 2017. Fine mapping of carbon assimilation rate 8, a quantitative trait locus for flag leaf nitrogen content, stomatal conductance and photosynthesis in rice. Frontiers in Plant Science **8**, 60.

Ainsworth EA. and Long SP. 2005. What have we learned from 15 years of free-air CO_2

enrichment (FACE)? A meta-analytic review of the responses of photosynthesis, canopy properties and plant production to rising CO_2. New Phytologist **165**, 351–372.

Ainsworth EA., Yendrek CR., Skoneczka JA. and Long SP. 2012. Accelerating yield potential in soybean: potential targets for biotechnological improvement. Plant, Cell & Environment **35**, 38–52.

Anderson I. and Backlund A. 2008. Structure and function of Rubisco. Plant Physiology and Biochemistry **46**, 275–291.

Barbour MM., Bachmann S., Bansal U., Bariana H., Sharp P. 2016. Genetic control of mesophyll conductance in common wheat. New Phytologist **209**, 461–465.

Bernacchi CJ., Singsaas EL., Pimentel C., Portis Jr AR., Long SP. 2001. Improved temperature response functions for models of Rubisco-limited photosynthesis. Plant, Cell & Environment **24**, 253–259.

Bernacchi CJ., Portis AR., Nakano H., von Caemmerer S., Long SP. 2002. Temperature response of mesophyll conductance. Implications for the determination of Rubisco enzyme kinetics and for limitations to photosynthesis in vivo. Plant Physiology **130**, 1992–1998.

Bernard RL. 1972**.** Two genes affecting stem termination in soybeans. Crop Science **12**, 235–239.

Bian JM., Jiang L., Liu LL. et al., 2010. Construction of a new set of rice chromosome segment substitution lines and identification of grain weight and related traits QTLs. Breeding Science **60**, 305–313.

Bradford MM. 1976. A rapid and sensitive method for the quantitation of microgram quantities of protein utilizing the principle of protein-dye binding. Analytical Biochemistry **72**, 248–254.

Brodribb TJ., Feild TS. and Jordan GJ. 2007. Leaf maximum photosynthetic rate and venation are linked by hydraulics. Plant Physiology **144**, 1890–1898.

Buttery BR. and Buzzell RI. 1977. The relationship between chlorophyll content and rate of photosynthesis in soybeans. Canadian Journal of Plant Science **57**, 1–5.

Buttery BR., Buzzell RI. and Findlay WI. 1981. Relationships among photosynthetic rate, bean yield and other characters in field-grown cultivars of soybean. Canadian Journal of Plant Science **61**, 191–198.

Caine RS., Yin X., Sloan J. et al., 2018. Rice with reduced stomatal density conserves water and has improved drought tolerance under future climate conditions. New Phytologist **221**, 371–384.

Caird MA., Richards JH. and Donovan LA. 2006. Nighttime stomatal conductance and transpiration in C_3 and C_4 plants. Plant Physiology **143**, 4–10.

Carmo-Silva AE. and Salvucci ME. 2012. The temperature response of CO_2 assimilation, photochemical activities and Rubisco activation in *Camelina sativa*, a potential bioenergy crop with limited capacity for acclimation to heat stress. Planta **236**,

1433–1445.

Carmo-Silva AE. and Salvucci ME. 2013. The regulatory properties of Rubisco activase differ among species and affect photosynthetic induction during light transitions. Plant Physiology **236**, 1433–1445.

Cheng L. and Fuchigami LH. 2000. Rubisco activation state decreases with increasing nitrogen content in apple leaves. Journal of Experimental Botany **51**, 1687–1694.

Concibido VC., La Vallee B., Mclaird P. et al., 2003. Introgression of a quantitative trait locus for yield from *Glycine soja* into commercial soybean cultivars. Theoretical and Applied Genetics **106**, 575–582.

Dornhoff GM. and Shibles RM. 1970. Varietal differences in net photosynthesis of soybean leaves. Crop Science **10**, 42–45.

Evans JR. 1983. Nitrogen and photosynthesis in the flag leaf of wheat (*Triticum aestivum* L.). Plant Physiology **72**, 297–302.

Evans JR. 1989. Photosynthesis and nitrogen relationships in leaves of C_3 plants. Oecologia **78**, 9–19.

Evans JR. 1999. Leaf anatomy enables more equal access to light and CO_2 between chloroplasts. New Phytologist **143**, 93–104.

Evans JR., Kaldenhoff R., Genty B., Terashima I. 2009. Resistances along the CO_2 diffusion pathway inside leaves. Journal of Experimental Botany **60**, 2235–2248.

Farquhar GD., von Cammerer S. and Berry JA. 1980. A biochemical model of photosynthetic CO_2 assimilation in leaves of C_3 species. Planta **149**, 78–90.

Farquhar GD. and Sharkey TD. 1982. Stomatal conductance and photosynthesis. Plant Physiology. **33**, 317–34.

Fischer RA., Rees D., Sayre KD., Lu ZM., Condon AG., Saavedra AL. 1998. Wheat yield progress associated with higher stomatal conductance and photosynthetic rate, and

cooler canopies. Crop Science **38**, 1467–1475.

Flexas J., Bota J., Loreto F., Cornic G., Sharkey TD. 2004. Diffusive and metabolic limitations to photosynthesis under drought and salinity in C_3 plants. Plant Biology **6**, 269–279.

Flexas J., Ribas-Carbo M., Hanson DT. et al., 2006. Tobacco aquaporin NtAQP1 is involved in mesophyll conductance to CO_2 in vivo. Plant Journal **48**, 427–439.

Flexas J., Ribas-Carbo M., Diaz-Espejo A., Galmes J., Medrano H. 2008. Mesophyll conductance to CO_2: current knowledge and future prospects. Plant, Cell & Environment **31**, 602–621.

Flexas J., Niinemets U., Galle A. et al., 2013. Diffusional conductances to CO_2 as a target for increasing photosynthesis and photosynthetic water-use efficiency. Photosynthesis Research **117**, 45–59.

Flood PJ., Harbinson J., Aarts MGM. 2011. Natural genetic variation in plant

Photosynthesis. Trends in Plant Science **16**, 327–335.

Food and Agriculture Organization of the United Nations. 2018. FAOSTAT. Food and Agriculture (Organization of the United Nations). http://www.fao.org/faostat/en/#home

von Caemmerer S. and Evans JR. 2010. Enhancing C_3 photosynthesis. Plant Physiology **154**, 589–592.

Franks PJ. and Beerling DJ. 2009. Maximum leaf conductance driven by CO_2 effects on stomatal size and density over geologic time. Proceedings of the National Academy of Science **106**, 10343–10347.

Fujita T., Noguchi K. and Terashima I. 2013. Apoplastic mesophyll signals induce rapid stomatal responses to CO_2 in *Commelina communis*. New Phytologist **199**, 395–406.

Fukayama H., Tamai T., Taniguchi Y. et al., 2006. Characterization and functional analysis of phosphoenolpyruvate carboxylase kinase genes in rice. The Plant Journal **47**,

258–268.

Fukayama H., Ueguchi C., Nishikawa K. et al., 2012. Overexpression of Rubisco activase decreases the photosynthetic CO_2 assimilation rate by reducing Rubisco content in rice leaves. Plant and Cell Physiology **53,** 976–986.

Guzman PS., Diers BW., Neece DJ. et al., 2006. QTL associated with yield in three backcross-derived populations of soybean. Crop Science **47**, 111–122.

Han Y., Li D., Zhu D. et al., 2012. QTL analysis of soybean seed weight across multi-genetic backgrounds and environments. Theoretical and Applied Genetics **125**, 671–683.

Hanba YT., Shibasaka M., Hayashi Y. et al., 2004. Aquaporin facilitated CO_2 permeation at the plasma membrane: over-expression of a barley aquaporin HvPIP2;1 enhanced internal CO_2 conductance and CO_2 assimilation in the leaves of the transgenic rice plant. Plant and Cell Physiology **45**, 521–529.

Harley PC., Loreto F., Di Marco G., Sharkey TD. 1992. Theoretical considerations when estimating the mesophyll conductance to CO_2 flux by analysis of the response of photosynthesis to CO_2. Plant Physiology **98**, 1429–1436.

Hashimoto-Sugimoto M., Higaki T., Yaeno T. et al., 2013. A Munc13-like protein in Arabidopsis mediates H+-ATPase translocation that is essential for stomatal responses. Nature Communications **4**, 1–7.

Hibberd JM., Sheehy JE. and Langdale JA. 2008. Using C_4 photosynthesis to increase the yield of rice-rationale and feasibility. Current Opinion in Plant Biology **11**, 228–231.

Hikosaka K. 2004. Interspecific difference in the photosynthesis-nitrogen relationship: Patterns, physiological causes, and ecological importance. Journal of Plant Research **117**, 481–494.

Hikosaka K. 2010. Mechanisms underlying interspecific variation in photosynthetic capacity across wild plant species. Plant Biotechnology **27**, 223–229.

Hu SP., Zhou Y., Zhang L. et al., 2009. Correlation and quantitative trait loci analyses of total chlorophyll content and photosynthetic rate of rice (*Oryza sativa*) under water stress and well-watered conditions. Journal of Integrative Plant Biology **51**, 879–888.

Inoue S. and Kinoshita T. 2017. Blue light regulation of stomatal opening and the plasma membrane H^+-ATPase. Plant Physiology **174**, 531–538.

IPCC. 2018. Carbon Dioxide: Projected emissions and concentrations. http://ipcc-data.org/observ/ddc_co2.html

Ishikawa C., Hatanaka T., Misoo S. et al., 2009. Screening of high k_{cat} Rubisco among Poaceae for improvement of photosynthetic CO_2 assimilation in rice. Plant Production Science **12**, 345–350.

Ishikawa C., Hatanaka T., Misoo S. et al., 2011. Functional incorporation of sorghum small subunit increases the catalytic turnover rate of Rubisco in transgenic rice. Plant Physiology **156**, 1603–1611.

Ishikawa-Sakurai J., Hayashi H. and Murai-Hatano M. 2014. Nitrogen availability affects hydraulic conductivity of rice roots, possibly through changes in aquaporin gene expression. Plant and Soil **379**, 289–300.

Jiang CZ., Rodermel SR. and Shibles RM. 1993. Photosynthesis, Rubisco activity and amount, and their regulation by transcription in senescing soybean leaves. Plant Physiology **101**, 105–112.

Jiang CJ., Quick WP., Alred R. et al., 1994. Antisense RNA inhibition of Rubisco activase expression. The Plant Journal **5**, 787–798.

Jin J., Liu X., Wang G. et al., 2010. Agronomic and physiological contributions to the yield improvement of soybean cultivars released from 1950 to 2006 in Northeast China. Field Crops Research **115**, 116–123.

Kabelka EA., Diers BW., Fehr AR. et al., 2004. Putative alleles for increased yield from soybean plant introductions. Crop Science **44**, 784–791.

Kanemura T., Homma K., Ohsumi A., Shiraiwa T. and Horie T. 2007. Evaluation of genotypic variation in leaf photosynthetic rate and its associated factors by using rice diversity research set of germplasm. Photosynthesis Research **94**, 23–30.

Kanno K., Suzuki Y. and Makino A. 2017. A small decrease in rubisco content by individual suppression of RBCS genes leads to improvement of photosynthesis and greater biomass production in rice under conditions of elevated CO_2. Plant and Cell Physiology **58**, 635–642.

Kawamitsu Y. and Agata W. 1987. Varietal differences in photosynthetic rate, transpiration rate and leaf conductance for leaves of rice plants. Japanese Journal of Crop Science **53**, 563–570.

Kawasaki Y., Tanaka Y., Katsura K. and Shiraiwa T. 2014. Dry matter production and nitrogen utilization of high yielding soybean cultivars. Poster presented at: Grand challenges: Great solutions. ASA, CSSA, and SSSA Annual Meetings, Long Beach, CA. 2–5 Nov. Poster 394–17.

Kawasaki Y., Tanaka Y., Katsura K., Purcell LC., Shiraiwa T. 2016. Yield and dry matter productivity of Japanese and US soybean cultivars. Plant Production Science **19**, 257–266.

Koester RP., Skoneczka JA., Cary TR., Diers BW., Ainsworth EA. 2014. Historical gains in soybean (*Glycine max* Merr.) seed yield are driven by linear increases in light interception, energy conversion, and partitioning efficiencies. Journal of Experimental Botany **65**, 3311–3321.

Koester RP, Nohl BM, Diers BW, Ainsworth EA. 2016. Has photosynthetic capacity increased with 80 years of soybean breeding? An examination of historical soybean cultivars. Plant, Cell & Environment **39**, 1058–1067.

Köhler IH., Ruiz-Vera UM., VanLoocke A. et al., 2017. Expression of cyanobacterial FBP/SBPase in soybean prevents yield depression under future climate conditions. Journal of Experimental Botany **68**, 715–726.

Kokubun M. and Shimada S. 1994a. Diurnal change of photosynthesis and its relation

to yield in soybean cultivars. Japanese Journal of Crop Science **63**, 305–312.

Kokubun M. and Shimada S. 1994b. Relation between midday depression of photosynthesis and leaf water status in soybean cultivars. Japanese Journal of Crop Science **63**, 643–649.

Kurata N., Nagamura Y., Yamamoto K. et al., 1994. A 300 kilobase interval genetic map of rice including 883 expressed sequences. Nature Biotechnology **8**, 365–372.

Lefebvre S., Lawson T., Zakhleniuk OV., Lloyd JC., Raines CA. 2005. Increased sedoheptulose-1,7-bisphosphatase activity in transgenic tobacco plants stimulates photosynthesis and growth from an early stage in development. Plant Physiology **138**, 451–460.

Li H., Yang Y., Zhang H. et al., 2016. A genetic relationship between phosphorus efficiency and photosynthetic traits in soybean as revealed by QTL analysis using a high-density genetic map. Frontiers in Plant Science **7**, 924.

Li X., Fang C., Xu M. et al., 2016. Quantitative trait locus mapping of soybean maturity gene *E6*. Crop Science **57**, 1–8.

Lieman-Hurwitz J., Rachmilevitch S., Mittler R., Marcus Y., Kaplan A. 2003. Enhanced photosynthesis and growth of transgenic plants that express *ictB*, a gene involved in HCO_3^- accumulation in cyanobacteria. Plant Biotechnology Journal **1**, 43–50.

Liu G., Yang C., Xu K. et al., 2012.Development of yield and some photosynthetic characteristics during 82 years of genetic improvement of soybean genotypes in northeast China. Australian Journal of Crop Science **57**, 1–8.

Long SP. 1998. Rubisco, the key to improved crop production for a world population of more than eight billion people? In Feeding a World Population of More Than Eight Billion People – A Challenge to Science (eds J.C. Waterlow, D.G. Armstrong, L. Fowdenand & R. Riley), 124–136. Oxford University Press, Cary, NC, USA.

Long SP, Zhu XG, Naidu SL, Ort DR. 2006. Can improvement in photosynthesis

increase crop yields? Plant, Cell & Environment **29**, 315–330.

Lu S., Zhao X., Hu Y. et al., 2017. Natural variation at the soybean J locus improves adaptation to the tropics and enhances yield. Nature Genetics **49**, 773–779.

Mächler F., Oberson A., Grub A., Nösberger J. 1988. Regulation of photosynthesis in nitrogen deficient wheat seedlings. Plant Physiology **87**, 46–49.

Makino A., Mae T. and Ohira K. 1985. Photosynthesis and ribulose-l,5-bisphosphate carboxylase/oxygenase in rice leaves from emergence through senescence. Quantitative analysis by carboxylation/oxygenation and regeneration of ribulose 1,5-bisphosphate. Planta **166**, 414–420.

Makino A., Mae T. and Ohira K. 1986. Colorimetric measurement of protein stained with Coomassie Brilliant Blue R on Sodium Dodecyl Sulfate-Polyacrylamide Gel Electrophoresis by Eluting with Formamide. Agricultural and Biological Chemistry **50**, 1911–1912.

Makino A., Mae T. and Ohira K. 1987. Variations in the contents and kinetic properties of ribulose-1,5-bisphosphate carboxylases among rice species. Plant and Cell Physiology **28**, 799–804.

Makino A., Shimada T., Takumi S. et al., 1997. Does decrease in ribulose-1,5-bisphosphate carboxylase by antisense RbcS lead to a higher N-use efficiency of photosynthesis under conditions of saturating CO_2 and light in rice plants? Plant Physiology **114**, 483–491.

Masuda T. and Goldsmith PD. 2009. World soybean production: Area harvested, yield, and long-term projections. World **12**, 143–162.

Mate CJ., Hudson GS., von Caemmerer S. et al., 1993. Reduction of ribulose bisphosphate carboxylase activase levels in tobacco (*Nicotiana tabacum*) by antisense RNA reduces ribulose bisphosphate carboxylase carbamylation and impairs photosynthesis. Plant Physiology **102**, 1119–1128.

Matthews JSA., Vialet-Chabrand SRM. and Lawson T. 2017. Diurnal variation in gas

exchange: The balance between carbon fixation and water loss. Plant Physiology **174**, 614–623.

McMurtrie RE. and Wang YP. 1993. Mathematical models of the photosynthetic response of tree stands to rising CO_2 concentrations and temperatures. Plant, Cell & Environment **16**, 1–13.

Mitchell RAC., Black CR., Burkart S., et al. 1999. Photosynthetic responses in spring wheat grown under elevated CO_2 concentrations and stress conditions in the European, multiple-site experiment 'ESPACE-wheat'. European Journal of Agronomy **10**, 205–214.

Monteith JL. 1977. Climate and the efficiency of crop production in Britain. Philosophical Transactions of the Royal Society of London **281**, 277–294.

Morrison MJ., Voldeng HD. and Cober ER. 2000. Physiological changes from 58 years of genetic improvement of short-season soybean cultivars in Canada. Agronomy Journal **91**, 685-689

Ohsumi A., Hamasaki A., Nakagawa H., Yoshida H., Shiraiwa T., Horie T. 2007. A model explaining genotypic and ontogenetic variation of leaf photosynthetic rate in rice (*Oryza sativa*) based on leaf nitrogen content and stomatal conductance. Annals of Botany **99**, 265–273.

Ojima M. 1972. Improvement of leaf photosynthesis in soybean varieties. The National Institute of Agricultural Sciences Bulletin Series D **23**, 97–154.

Orf JH., Chase K., Adler FR., Mansur LM., Lark KG. 1999. Genetics of soybean agronomic traits: II. interactions between yield quantitative trait loci in soybean. Crop Science **39**, 1652–1657.

Perdomo JA., Capo-Bauca S., Carmo-Silva E. et al., 2017. Rubisco and Rubisco activase play an important role in the biochemical limitations of photosynthesis in rice, wheat, and maize under high temperature and water deficit. Frontiers in Plant Science **8**, 490.

Pons T., L. Flexas J., von Caemmerer S. et al., 2009. Estimating mesophyll conductance to CO2: methodology, potential errors, and recommendations. Journal of Experimental Botany **60**, 2217–2234.

Porra RJ., Thompson WA. and Kriedemann PE. 1989. Determination of accurate extinction coefficients and simultaneous equations for assaying chlorophylls a and b extracted with four different solvents: verification of the concentration of chlorophyll standards by atomic absorption spectroscopy. Biochimica et Biophysica Acta (BBA). Bioenergetics **975**, 384–394.

Portis AR. 1992. Regulation of ribulose-1,5-bisphosphate carboxylase/oxygenase activity. Annual Review of Plant Physiology **43**, 415–437.

Portis AR. 2003. Rubisco activase Rubisco's catalytic chaperone. Photosynthesis Research **75**, 11–27.

Quick WP., Schurr U., Scheibe R. et al., 1991. Decreased ribulose-l,5-bisphosphate carboxylase-oxygenase in transgenic tobacco transformed with "antisense" rbcS. I.

Impact on photosynthesis in ambient growth conditions. Planta **183**, 542–554.

Radin JW., Parker LL. and Guinn G. 1982. Water relations of cotton plants under nitrogen deficiency. Plant Physiology **70**, 1066–1070.

Raines CA. 2011. Increasing Photosynthetic Carbon Assimilation in C_3 Plants to Improve Crop Yield: Current and Future Strategies. Plant Physiology **155**, 36–42.

Ray JD., Dhanapal AP., Singh SK. et al., 2015. Genome-wide association study of ureide concentration in diverse maturity group IV soybean [*Glycine max* (L.) Merr.] accessions. G3: Genes/ Genomes/ Genetics **5**, 2391–2403.

Sakoda K., Tanaka Y., Long SP., Shiraiwa T. 2016. Genetic and physiological diversity in the leaf photosynthetic capacity of soybean. Crop Science **56**, 2731–2741.

Schlüter U., Muschak M., Berger D., Altmann T. 2003. Photosynthetic performance of an Arabidopsis mutant with elevated stomatal density (*sdd1-1*) under different light regimes. Journal of Experimental Botany **54**, 867–874.

Schneider CA., Rasband WS. and Eliceiri KW. 2012. NIH Image to ImageJ: 25 years of image analysis. Nature Methods **9**, 671–675.

Servaites JC., Shieh WJ. and Geiger DR. 1991. Regulation of photosynthetic carbon reduction cycle by Ribulose bisphosphate and Phosphoglyceric acid. Plant Physiology **97**, 1115–1121.

Sharkey TD. 1982. Stomatal conductance and photosynthesis. Annual Review of Plant Physiology **33**, 317–345.

Sharkey TD. 1985. Photosynthesis in intact leaves of C_3 plants: Physics, physiology and rate limitations. The Botanical Review **51**, 53–105.

Sinclair TR. and Horie T. 1989. Leaf nitrogen, photosynthesis, and crop radiation use efficiency: A review. Crop Science **29**, 90–98.

Soleh MA., Tanaka Y., Nomoto Y. et al., 2015. Factors underlying genotypic differences

in the induction of photosynthesis in soybean [*Glycine max* (L.) Merr.]. Plant, Cell & Environment **39**, 685–693.

Specht JE., Hume DJ. And Kumudini SV. 1999. Soybean yield potential–A genetic and physiological perspective. Crop Science **39**, 1560–1570.

Suzuki Y., Ohkubo M., Hatakeyama H. et al., 2007. Increased Rubisco content in transgenic rice transformed with the 'sense' rbcS gene. Plant and Cell Physiology **48**, 626–637.

Suzuki Y., Fujimori T., Kanno K. et al., 2012. Metabolome analysis of photosynthesis and the related primary metabolites in the leaves of transgenic rice plants with increased or decreased Rubisco content. Plant, Cell & Environment **35**, 1369–1379.

Takai T., Adachi S., Taguchi-Shiobara F., et al. 2013. A natural variant of *NAL1*, selected in high-yield rice breeding programs, pleiotropically increases photosynthesis rate. Scientific Reports **3**, 2149.

Takai T, Ikka T, Kondo K. et al., 2014. Genetic mechanisms underlying yield potential in the rice high-yielding cultivar Takanari, based on reciprocal chromosome segment substitution lines. BMC Plant Biology **14**, 295.

Tanaka Y., Shiraiwa T., Nakajima A., Sato J., Nakazaki T. 2008. Leaf gas exchange activity in soybean as related to leaf traits and stem growth habit. Crop Science **48**, 1925–1932.

Tanaka Y. and Shiraiwa T. 2009. Stem growth habit affects leaf morphology and gas exchange traits in soybean. Annals of Botany **104**, 1293–1299.

Tanaka Y., Fujii K. and Shiraiwa T. 2010. Variability of leaf morphology and stomatal conductance in soybean [*Glycine max* (L.) Merr.] cultivars. Crop Science **50**, 2525–2532.

Tanaka Y., Fukuda Y., Nakashima K. and Shiraiwa T. 2013a. High-throughput phenotyping of the leaf transpiration at the primary leaf in soybean [*Glycine max* (L.) Merr.]. Poster presented at: Water, Food, Energy & Innovation for a Sustainable World. ASA, CSSA, and SSSA Annual Meetings, Tampa, Florida. 3–6 Nov. Poster 370-13.

Tanaka Y., Sugano SS., Shimada T., Hara-Nishimura I. 2013b. Enhancement of leaf photosynthetic capacity through increased stomatal density in Arabidopsis. New Phytologist **198**, 757–764.

Taylor SH. and Long SP. 2017. Slow induction of photosynthesis on shade to sun transitions in wheat may cost at least 21% of productivity. Philosophical Transactions of the Royal Society B: Biological Sciences **372**, 1730.

Teng S., Qiand Q., Zeng D. et al., 2004. QTL analysis of leaf photosynthetic rate and related physiological traits in rice (*Oryza sativa* L.). Euphytica **135**, 1–7.

Tomeo NJ. and Rosenthal DM. 2017. Variable mesophyll conductance among soybean cultivars sets a tradeoff between photosynthesis and water-use-efficiency. Plant Physiology **174**, 241–257.

USCB. 2018. World Population 1950-2050. International Database (Washing- ton, DC: U.S. Department of Commerce, Census Bureau). http://www.census.gov/population/international/data/idb/worldpopgraph.php

USDA. 2012. Soybeans and Oil crops: Overview. USDA Economic Research Service. http://www.ers.usda.gov/topics/crops/soybeans-oil-crops.aspx

Vickery HB. 1946. The early years of the Kjeldahl Method to determine nitrogen. Yale Journal of Biology and Medicine **18,** 473–514.

Vieira AJD., Oliveira DA., Soares TCB., et al. 2006. Use of the QTL approach to the study of soybean trait relationships in two populations of recombinant inbred lines at the F_7 and F_8 generations. Brazilian Journal of Plant Physiology **18**, 281–290.

Walker BJ. and Ort DR. 2015. Improved method for measuring the apparent CO_2 photocompensation point resolves the impact of multiple internal conductances to CO_2 to net gas exchange. Plant, Cell & Environment **38**, 2462–2474.

Wang P., Xing Y., Li Z., Yu S. 2012. Improving rice yield and quality by QTL pyramiding. Molecular Breeding **29**, 903–913.

Wang W., He Q., Yang H., Xiang S., Zhao T., Gai J. 2013. Development of a chromosome segment substitution line population with wild soybean (*Glycine soja* Sieb. et Zucc.) as donor parent. Euphytica **189**, 293–307.

Wang X., Pang Y., Zhang J. et al., 2014. Genetic background effects on QTL and QTL × environment interaction for yield and its component traits as revealed by reciprocal introgression lines in rice. The Crop Journal **2**, 345–357.

Wang Y., Noguchi K., Ono N., Inoue S., Terashima I., Kinoshita T. 2014. Overexpression of plasma membrane H^+-ATPase in guard cells promotes light-induced stomatal opening and enhances plant growth. Proceedings of the National Academy of Sciences **111**, 533–538.

Watanabe S., Harada K. and Abe J. 2012. Genetic and molecular bases of photoperiod responses of flowering in soybean. Breeding Science **61**, 531–543.

Watanabe S., Shimizu T., Machita K. et al., 2018. Development of a high-density linkage map and chromosome segment substitution lines for Japanese soybean cultivar Enrei. DNA Research **25**, 213–136.

Whitney SM., Houtz RL. and Alonso H. 2011. Advancing our understanding and capacity to engineer nature's CO_2-sequestering enzyme, Rubisco. Plant Physiology **155**, 27–35.

Xiong D., Yu T., Zhang T. et al., 2015. Leaf hydraulic conductance is coordinated with leaf morpho-anatomical traits and nitrogen status in the genus *Oryza*. Journal of Experimental Botany **66**, 741–748.

Xin D., Qi Z., Jiang H. et al., 2016. QTL location and epistatic effect analysis of 100-seed weight using wild soybean (*Glycine soja* Sieb. & Zucc.) chromosome segment substitution lines. PLoS ONE **11**, e0149380.

Yamori W., Masumoto C., Fukayama H., Makino A. 2012. Rubisco activase is a key regulator of non-steady-state photosynthesis at any leaf temperature and, to a lesser extent, of steady-state photosynthesis at high temperature. The Plant Journal **71**, 871–880.

Yano M. 2001. Genetic and molecular dissection of naturally occurring variation. Current Opinion in Plant Biology **4**, 130–135.

Yin Z., Meng F., Song H., He X., Xu X., Yu D. 2010. Mapping quantitative trait loci associated with chlorophyll a fluorescence parameters in soybean (*Glycine max* (L.) Merr.). Planta **231**, 875–885.

Yoshimura Y. and Kubota F. 2000. Estimation of vein length in a leaf of sweet potato (*Ipomoea batatas Lam.*) by the lattice crossing method. Japanese Journal of Crop Science **69**, 92–94.

Yuan J., Njiti VN., Meksem K. et al., 2002. Quantitative trait loci in two soybean recombinant inbred line populations segregating for yield and disease resistance. Crop Science **42**, 271–277.

Zhang N., Kallis RP., Ewy RG. et al., 2002. Light modulation of Rubisco in Arabidopsis requires a capacity for redox regulation of the larger Rubisco activase isoform. Proceedings of the National Academy of Sciences **99**, 3330–3334.

Zhu X., de Sturler E. and Long SP. 2007. Optimizing the distribution of resources between enzymes of carbon metabolism can dramatically increase photosynthetic rate: A numerical simulation using an evolutionary algorithm. Plant Physiology **145**, 513–526.

Zhu XG., Long SP. and Ort DR. 2010. Improving photosynthetic efficiency for greater yield. Annual Review of Plant Biology **61**, 235–261.

List of publications

(Chapter 2 and 3)

Sakoda K., Tanaka Y., Long SP. and Shiraiwa T. 2016. Genetic and Physiological Diversity in the Leaf Photosynthetic Capacity of Soybeans. Crop Science **56**, 2731–2741.

(Chapter 2 and 3)

Sakoda K., Suzuki S., Fukayama H., Tanaka Y. and Shiraiwa T. Activation State of Rubisco Decreases with the Nitrogen accumulation during the Reproductive Stage in Soybean [*Glycine max* (L.) Merr.]. Photosynthetica (in press)

(Chapter 4)

Sakoda K., Kaga A., Tanaka Y., Suzuki S., Fujii K., Ishimoto M. and Shiraiwa T. Two Novel Quantitative Trait Loci Affecting the Variation in Leaf Photosynthetic Capacity among Soybeans. (Under submission)